Networks and Heterogeneous Media

NHM, 21(4): 1227–1261.
DOI: 10.3934/nhm.2026049
Received: 30 January 2026
Revised: 23 May 2026
Accepted: 16 June 2026
Published: 26 June 2026

https://www.aimspress.com/journal/NHM

Research article

Dispersion of periodic flows on the surface of a viscous heterogeneous liquid

Yuli D. Chashechkin* **and Artem A. Ochirov**

Laboratory of Fluid Mechanics, Ishlinsky Institute for Problems in Mechanics RAS, Prospekt Vernadskogo, 101-1, Moscow 119526, Russia

* **Correspondence:** Email: yulidch@gmail.com; Tel: +74954340192.

Abstract: Periodic capillary-gravitational perturbations propagating along the free surface of a heterogeneous liquid were investigated by methods of united perturbation theory. A reduced system of heterogeneous fluid mechanics equations, which takes into account the non-uniformity of the liquid density distribution without considering the physical nature of stratification, was analyzed. The methods of the united theory of regular and singular perturbations in linear approximation were employed to obtain complete dispersion relations that describe the large-scale dynamics and fine structure of periodic flows. Analysis of solution showed that calculated regular functions characterize wave components that determine the large-scale geometry and flow dynamics. Singular functions describe ligament components that determine the fine structure of flows. Moreover, the basic properties of large-scale wave components and ligament fine-structured components were calculated for a liquid with water parameters and different values of the buoyancy frequency in an exponentially stratified liquid. When performing the limiting transition to simpler models, the relations obtained uniformly converged to known expressions for capillary-gravity and internal waves. Singular solutions were lost when the effects of viscosity were neglected in a stratified and homogeneous liquid. A substantial difference of the first constructed complete dispersion relation for periodic gravity–capillary flows from that previously obtained using the Boussinesq approximation is shown.

Keywords: system of fundamental equations; ligaments; waves; dispersion relations; complete solutions; stratification; viscosity; free surface

1. Introduction

Systematic measurements of the fundamental physical quantity distributions, i.e., temperature T, concentration of dissolved impurities or suspended particles S_i, and pressure P, have been carried out in fluids and gases since the middle of the last century. They have shown that all quantities, including the density, which is determined by the equation of state, in technological installations and in natural and laboratory conditions are unevenly distributed.

In nature, all media, both liquid and gaseous, are heterogeneous; their state is constantly changing under the influence of atomic, molecular, and external factors. In a gravitational field with free fall acceleration g, light particles float and heavy particles submerge and form a stable density distribution with depth that is stratification of hydrosphere with depth or with height in the atmosphere $\rho(z)$. Stratification is characterized by the length scale $\Lambda = \left| \frac{1}{\rho(z)} \frac{d\rho(z)}{dz} \right|^{-1}$, frequency $N = \sqrt{g/\Lambda}$, and buoyancy period $T_b = 2\pi/N$, locally and in general.

Precision measurements have also revealed that the hydrosphere and atmosphere have a fine structure, in which thick, more homogeneous layers are separated by thin interfaces with high-gradients of physical quantities [1–3]. Natural processes of molecular diffusion of matter and thermal conductivity violate the medium stationary conditions and generate thin non-stationary boundary “flows induced by diffusion” [4,5]. They compensate for the lack or excess of substance near impenetrable inclined boundaries. Experiments have shown that sharp density inhomogeneities occur in a moving medium and in a medium at rest [6].

Typical quantities of the intrinsic time and length scales of stratified media with dynamic μ and kinematic viscosity $\nu = \mu/\rho$ are shown in Table 1. All media are divided into four categories. Highly stratified liquid or gas with a buoyancy period $3 < T_b < 20$ s can be found in laboratory installations. Weakly stratified liquid or gas (in this classification) with a buoyancy period in the range of $3 < T_b < 30$ min is observed in an ocean [1] and compressible atmosphere [2,3].

A potentially homogeneous fluid with a buoyancy period of the order of several days is a physically justified model of a “uniform” medium. Due to the smallness, the density variations of this medium are not directly registered by modern tools. The fact that confirms the universality of its existence is the “fine structure” of this medium. It consists of thin interfaces and fibers with unique properties. These interfaces are registered by sensitive optical methods in flows of fluids and gases in the laboratory [7] and natural environment [1,3].

The generation of “fine structures” is provided by the dynamics of the components of microstructural associates (“grains”, “cells”), such as complexes, clathrates, clusters, voids, and bonds. They are created due to the anisotropy of atomic and molecular properties of substances stimulating their formation [8,9]. The boundaries of elements and free surfaces are characterized by the potential surface energy (PSE), which is included in the Gibbs potential selected for the description of the internal energy of a continuous medium [10,11].

Table 1. Typical quantities of parameters in the natural environment.

Parameter	Medium							
	Stratified				Homogeneous			
	Highly		Weakly		Potentially		Actually	
	Air	Water	Air	Water	Air	Water	Air	Water
N, c^{-1}—buoyancy frequency	1		0.01		10^{-5}		0	
T_b—buoyancy period	10 s		10 min		10 days		∞	
Λ—stratification scale	10 m		100 km		10^8 km		∞	
$\delta_N^{g\nu} = (g\nu)^{1/3} N^{-1}$, cm—combined Rayleigh scale	5	2	500	200	5×10^5	2×10^5	∞	
$\delta_N^{\nu} = \sqrt{\nu/N}$, cm—Rayleigh microscale	0.4	0.1	4	1	120	30	∞	

The energy that is needed for the creation of cell boundaries and contact surface is extracted during the formation of the elements from the medium thermal energy and the kinetic energy of the flow. PSE is released during the decay or restructuring of the cell pattern and is transferred into the perturbations of thermodynamic quantities, such as temperature, pressure, and impurity concentrations, as well as the thinnest flow components [12]. Associates, existing in the thickness of continuous media and at the contact boundaries of liquids and gases, are continuously created, transformed, and disintegrated. Generated fine flow components ensure zero static friction of fluids and gases. The images of the structured photosphere of the Sun, in which the average value of the buoyancy period and the duration of the existence of individual cells are of the order of ten minutes, serve as a universal optical representation of the any fluid medium micro-granular structure [13].

Throughout the history of theoretical and applied mechanics of fluids and gases, the consideration of density variability and determination of its dependence on other values are outlined. Euler's fundamental research includes the derivation of the first system of equations for the mechanics of an ideal fluid. In the preface of his paper, L. Euler emphasized the importance of taking into account the influence of heat and other physical factors (determining the density of a medium) on the dynamics of flows [14]. G. G. Stokes also gave significant attention to the discussion of the medium heterogeneity role in the derivation of equations of fluid mechanics. However, the level of mathematical development in the 19th century made G. G. Stokes recognize «As it is quite useless to consider cases of the utmost degree of generality, I shall suppose the fluid to be homogeneous…» [15]. It also predetermined the predominant choice of approximation for a homogeneous medium in the subsequent evolution of the theory of waves and flows [16,17].

Later, G. G. Stokes again emphasized the limitations of the formulated theory of flows during the construction of the solutions of obtained equations: «The three equations of which (l) is the type are not the general equations of motion which apply to a heterogeneous fluid when internal friction is taken into account, which are those numbered (10) in my former paper, but are applicable to a homogeneous incompressible fluid, or to a homogeneous elastic fluid subject to small variations of density, such as those which accompany sonorous vibrations» [18]. He additionally considered the problem of wave propagation in a layered fluid [19].

Furthermore, some prominent mathematicians continued to develop the theory of flows and waves in heterogeneous fluids. H. Lamb included references [20] to the first observations of the effect of stratification on fluid oscillations in ship lamp [21] and a series of remarkable experiments by V. Ekman [22]. These experiments included the modeling of the vessel "Fram" movement, aboard which F. Nansen met the phenomenon of "dead water" in Norwegian fjords and the Kara Sea, in the basin with a stratified fluid [22]. The consideration of oscillations in continuously stratified fluid and the determination of the cutoff frequency that is limiting frequency of traveling internal waves is presented in [23]. The cutoff frequency was later defined experimentally as the frequency of natural oscillations of meteorological balloons in the atmosphere [24]. Later, local maxima in the spectra of micro barometric perturbations at the cutoff frequency was identified [25]. Theoretical studies of oscillations and waves in a stratified atmosphere were continued by H. Lamb at the beginning of the last century [26].

The emergence of popular monographs that contain the results of theoretical research on waves [27] and generalizing data from exploratory experimental studies [6] were the evidence of the renewed interest in investigating the effects of heterogeneity and stratification after a long break. Gradually, two approaches were distinguished among the unique studies, reviews, and monographs on the effects of stratification. They were the traditional approach, which was based on the examination of regular solutions, and the generalized approach, which took into account the singular properties of a system of fundamental equations for heterogeneous fluids.

In the traditional approach, a linearized system of Euler or Navier–Stokes equations with a predetermined unperturbed density distribution is chosen as the basis for studying acoustic, gravitational, surface, internal waves, and other types of waves [17,27,28]. To simplify calculations, the Boussinesq approximation is employed, in which small density variations are preserved only in terms with large coefficients. Periodic solutions were obtained by the regular perturbation theory, the foundations of which were laid in G. G. Stokes, Rayleigh, H. Poincaré, and A. M. Lyapunov. To account for dissipative effects, a factor describing the exponential attenuation of the amplitude as the wave propagates was included into the solutions of the Euler equations [28].

An alternative approach is based on the analysis of a complete system of equations describing the mechanics of heterogeneous fluids. The system (or its reduced forms, excluding the equations of heat transfer (temperature) and impurity concentration) includes the equation of state for density [12,27]. The analysis is carried out by methods of the united theory of regular and singular perturbations [29]. The presence of small coefficients in terms with higher derivatives enables constructing the complete analytic solutions of the equations system. They involve regular solutions obtained by methods of traditional perturbation theory [30], and additional solutions obtained by the application of the theory of singular perturbations [29]. Thin interfaces in intersection domain beams of smooth periodic internal wave beams in a continuously stratified fluid corresponding to the singular solutions, were previously visualized in several high-resolution experiments [30,31].

The relations of large (buoyancy scale) and small (included kinematic viscosity) length scales to the geometry parameters of the problem were used in the construction of new classes of solutions. Initially, these new classes of solutions were obtained during the investigation of the periodic flows generation in the thickness of a continuously stratified fluid [32]. The comparison with data of schlieren visualization of stratified flows showed that the regular parts of the received complete solutions describe beams of the periodic internal waves. Singular components (ligaments) characterize the fine structure that occur in the fields of internal waves in an originally continuously stratified liquid [33]; the term "ligament" was borrowed by Rayleigh [34] from medicine, where it is used as a synonym of fibrous connective tissues that bind organs or connect heterogeneous body parts, e.g., bones with bones and bones with muscles. The general properties of singular components, which complement the known types of waves (inertial, gravitational, acoustic and hybrid), were analyzed in [35].

Periodic internal wave beams partially leak into the forbidden domain in a liquid with a varying density profile and are reflected from a critical layer where the buoyancy and falling wave frequencies coincide [36]. The calculation results for the parameters of these beams are consistent with the data of later performed experiments [37], within a few percent.

The theory of waves on the fluid surface has important practical significance. Their theoretical study is traditionally carried out in the approximation of homogeneous fluid. A rigorous mathematical description of surface waves began with G. B. Airy's studies [38], who developed the first theory of linear waves, which is considered the basis of oceanographic research. The foundations of nonlinear theory were established in the article by G. G. Stokes [19].

At the end of the 19th century, the first generalizing treatise appeared, which described the surface linear and nonlinear wave motions in detail [20]. Later, this treatise was supplemented by a variety of monographs describing waves in deep and shallow fluids. At the beginning of the 20th century, classic monographs appeared that systematically presented the mathematical theory of waves on the surface of a heavy fluid, including gravitational and capillary waves [27,39]. Later, researchers emerged who examined the linear and nonlinear theory of waves [40], scrutinized processes in the ocean surface layer in detail [41], and comprehensively described all types of waves encountered in the ocean [42]. Applied research aimed at engineering applications began to appear, such as wave transformation in the coastal zone [43], nonlinear interactions, and the influence of bottom topography in deep and shallow water [44,45]. The influence of the underlying surface on the propagation of surface waves was investigated in some studies [46]. The theory of wave interaction on the fluid surface was also actively developed [47]. A considerable number of researchers were dedicated to obtaining accurate analytical solutions for linear problems of wave interaction with various barriers. The influence of vertical [48,49] and horizontal [50] barriers on wave motion in deep water was investigated. Scattering problems on solid and porous barriers [51,52] were considered.

A set of analytical solutions for waves generated by landslides, including free surface elevations and velocity fields, are shown in [53]. Analytical solutions for the diffraction of water waves on vertical truncated cylinders within the framework of linear potential theory were established in [54]. The effect of viscosity on steep surface waves was assessed by a time-dependent conformal method in [55]. The asymptotic behavior of the Green function in the linearized Navier–Stokes equations for a compressible fluid was investigated in [56]. The authors applied weighted energy estimate and long wave-short wave decomposition to study the behavior of the Green function and its decomposition when calculating wave components. They also gave much attention to the problems of interaction between a fluid and solid inclusions, which create suspensions and polymer solutions [57,58].

The development of the nonlinear surface wave theory is a dynamic direction of modern research of a homogeneous fluid dynamics. New two-dimensional horizontal flow models with a free surface are shown in [59]. The study of nonlinear focusing on standing waves was carried out in [60]. The evolution of nonlinear wind waves was traced in [61]. Nonlinear surface waves could generate vorticity, as shown in [62].

Surface waves were also investigated in relation to their impact on subsurface gravity flows in a stratified ocean [63,64]. They play a significant role in the pollution propagation in the world ocean.

With the advancement of programming, more attention is given to the design of numerical methods, evaluating the impact of various factors on periodic flows on the surface and in the thickness of heterogeneous continuous media. A two-phase flow model in porous media that takes into account compressibility and viscosity was considered in [65]. A numerical scheme for applying the weak Bubnov–Galerkin technique was developed in [66], where the existence and uniqueness of a weak numerical solution for the Navier-Stokes equations with damping were proved. A combined numerical scheme of methods for finite volumes and finite elements was proposed in [67] to solve the problems related to the propagation of dispersive waves in shallow water.

Analytical asymptotic methods are also being actively developed. At the end of the 20th century, the homotopy perturbation method was used to solve problems in hydrodynamics [68], which makes it possible to obtain solutions to problems in complex formulations in the approximation of a liquid of constant density (see for example [69,70]). Studies of the flow of a homogeneous incompressible fluid in a low viscosity approximation in a curved, three-dimensional domain with permeable walls were conducted in [71]. A numerical analysis of the surface tension influence on the growth of wind waves in an air-water system was performed in [72]. Numerical methods were employed to predict the behavior of waves on the ocean surface to forecast the impact on the movement of unmanned aerial vehicles [73]. In recent years, researchers have attempted to apply deep learning techniques for neural networks to evaluate the effect of surface waves on basic physical parameters of ocean such as temperature and salinity [74].

With some delay, methods for constructing complete solutions to the system of fundamental equations of heterogeneous fluid mechanics in linear and weakly nonlinear approximations began to be employed while investigating the propagation of periodic flows on the stratified fluid surface. Ligament solutions, which describe the fine structure of the physical fluid variables, emerge in a viscous liquid in addition to wave solutions. The increase in the order of the system of equations and the number of roots is due to the consideration of the ratio dispersion index, which determines the root number. Dispersion relations for all components of surface perturbations were first obtained in [75], where regular roots and singular ones were identified. Considering compressibility does not qualitatively change the solution in a two-dimensional formulation when a specific type of state equation is not taken into account.

The influence of surface electric charge on the character, dynamics, and structure of the components of periodic surface perturbations in stratified fluids applying the theory of singular perturbations was investigated in [76]. It is acceptable to use electrostatic approximation for an ideally conducting fluid or a liquid in which the relaxation time of the electric charge is much shorter than the characteristic time scales of periodic processes (i.e., the charge is accumulated near the fluid surface). Thus, the order of the system of equations describing the propagation phenomena of surface periodic flows remains unchanged, and the solution does not qualitatively differ from the case with an uncharged fluid. In this model, the surface electric charge has only a quantitative effect on the dispersion characteristics of the periodic flow components.

Our aim of this research is to construct complete analytical solutions for a reduced system of fundamental fluid mechanics equations that describe the propagation of surface two-dimensional perturbations without using simplifying Boussinesq approximation. Complete solutions containing regular flow components and singular components are searched in linear approximation. Many fluids in natural conditions have low viscosity or weak stratification, leading to the emergence of small parameters in terms with highest derivatives in the fundamental equations of heterogeneous liquid mechanics. This fact enables the employment of the united asymptotic techniques of the theory of regular and singular perturbations [29,77] to search solutions analytically. The fact that the frequencies of the propagating internal waves do not exceed the buoyancy frequency is considered [23].

This article contains several sections. In Section 2.1, the fundamental system of equations for the heterogeneous fluid mechanics properties and the limitations of model applicability are discussed. In Section 2.2, we consider the fundamental system in a reduced form, taking into account fluid stratification for two-dimensional periodic flows of viscous incompressible fluid. In Section 2.3, we dwell on the registration of physically-substantiated boundary conditions for surface wave propagation in a stratified ocean. Here, an analytical solution for the linearized problem with the commonly applied Boussinesq approximation is presented. The limitations of the model compared to the full formulation are also investigated. In Sections 2.4 and 2.5, we focus on solutions obtained in the ideal fluid model, with and without the Boussinesq approximation, correspondingly. Section 3 is devoted to the discussion of the results, types of dispersion relations in models, and comparison of the basic parameters of solutions in different approximations.

2. Problem formulation, methods and solution

2.1. System of fundamental fluid mechanics equations

When considering mathematical models of periodic flows in heterogeneous liquids, it is important to pay special attention to density determination.

The density of real liquids and gases is a complex value of mechanical, thermodynamic, and physical nature. Its connection with the thermodynamic parameters of a problem is taken into account in the state equation, which should be included in the system of equations that define the mathematical model [12,17]. However, the model of a constant-density liquid is widely used in theoretical wave studies [15]. It has no physical counterparts due to the atomic and molecular nature of substances and the formation of supramolecular associates [8,9]. When the homogeneous fluid model is employed, density being a constant coefficient is reduced in the equations of motion and is not considered when constructing solutions.

In heterogeneous liquids found in nature, there are distributions and fluctuations in temperature, pressure, and concentration of impurities. Therefore, it is important to consider the transfer of these values when creating a mathematical model. Fluids are structured and are compositions of different structural micro-components. During their disintegration and emergence, the energy is converted. To consider these processes when creating a mathematical model, the energy balance equation should be recorded along with the momentum transfer equation and continuity equation. The fundamental system of fluid mechanics equations [12,17,78] will be as follows:

$$\begin{gathered}
G = G\left(P, S, s_n, T\right), \qquad \rho = \rho\left(P, S, s_n, T\right), \\
\partial_t \rho + \nabla_j \left(p^j\right) = Q_\rho, \\
\partial_t \left(p^i\right) + \nabla_j \Pi^{ij} = \rho g^i + 2\varepsilon^{ijk} p_j \Omega_k + Q^i, \\
\partial_t \left(\rho T\right) + \nabla_j \left(p^j T\right) = \Delta\left(\kappa_T \rho T\right) + Q_T, \\
\partial_t \left(\rho s_n\right) + \nabla_j \left(p^j s_n\right) = \Delta\left(\kappa_s \rho s_n\right) + Q_{s_n}.
\end{gathered} \tag{2.1}$$

Here, G is Gibbs potential, symbol P denotes pressure, S stands for entropy, s_n denotes salinity of the n-th impurity, T stands for temperature, $Q_\rho, Q^i, Q_T, Q_{s_n}$ stand for the source of mass, momentum, temperature and the salinity concentration, respectively, $\mathbf{p}$ denotes momentum, $\Pi^{ij} = \rho u^i u^j + P\delta^{ij} - \sigma^{ij}$ stands for the momentum flux density tensor, u^i is the components of the fluid velocity $\mathbf{u} = \mathbf{p}/\rho$, ρ is density, δ^{ij} is the Kronecker delta, $\sigma^{ij} = \mu\left(\frac{\partial u^i}{\partial x^j} + \frac{\partial u^j}{\partial x^i} - \frac{2}{3}\delta^{ij}\frac{\partial u^k}{\partial x^k}\right) + \zeta\delta^{ij}\frac{\partial u^k}{\partial x^k}$ denotes the viscous stress tensor, μ, ζ are dynamic and bulk viscosities respectively, $\mathbf{g}$ is the gravity acceleration, ε^{ijk} is the Levi-Civita symbol, $\mathbf{\Omega}$ is the global rotation angular velocity, and κ_T, κ_{s_n} stand for thermal and mass diffusivity respectively.

Equation (2.1) has a high order and a corresponding number of solutions. In addition, the basic equations are supplemented by physically substantiated initial and boundary conditions. The non-leakage and adhesion conditions are recorded on solid surface, and kinematic and dynamic conditions should be recorded on a free surface. The absence of flow condition on boundary surfaces is also written [12,17,78]:

$$\mathbf{u}\big|_\Sigma = 0,\ \mathbf{u}\big|_{t\le 0} = 0,\ P\big|_{t\le 0} = P_0,\ \frac{\partial s_n}{\partial \mathbf{n}}\bigg|_\Sigma = 0,\ \frac{\partial T}{\partial \mathbf{n}}\bigg|_\Sigma = 0, s_n\big|_{t\le 0} = s_{n0},\ T\big|_{t\le 0} = T_0. \tag{2.2}$$

The system of Eq (2.1) is solved along with physically substantiated boundary conditions in Eq (2.2). The complete solutions to Eqs (2.1) and (2.2) determine all the components of periodic flows. However, Eqs (2.1) and (2.2) are too complex for analytical analysis, so to obtain analytical solutions, one has to simplify the model. These simplifications lead to a reduction in the order of the system, which in turn decreases the number of solutions and, consequently, the components of periodic flows. This fact should be taken into account when constructing mathematical models that describe the physical processes of flow generation and propagation in continuous heterogeneous media.

2.2. Mathematical problem formulation

In this paper, we investigate capillary-gravitational periodic flows that propagate along the free surface of an unbounded infinitely deep, incompressible stratified liquid in a two-dimensional (2D) formulation. The analysis is conducted in the Cartesian coordinate frame Oxz. Axis Ox corresponds to the equilibrium position of fluid free surface, along which the periodic perturbation $\zeta = \zeta(x,t)$ propagates. Axis Oz is directed vertically upward, opposite to the direction of gravity acceleration $\mathbf{g}$. To simplify the mathematical derivations, an exponentially density-stratified fluid is used. In nature, stratification is governed by variations in temperature or the concentration of dissolved substances. In this work, following the classical studies [27], a problem of mechanics is considered, and the physical nature of the stratification is not analyzed. We accept that the velocity field is solenoidal. With regard to that mentioned above, the mathematical formulation of the problem can be written as follows [76]:

$$\begin{aligned}
&\rho\left(\partial_t \mathbf{u} + (\mathbf{u}\cdot\nabla)\mathbf{u}\right) = \rho\nu\Delta\mathbf{u} - \nabla P + \rho\mathbf{g},\\
&\partial_t\rho + \nabla(\rho\mathbf{u}) = 0,\\
&\rho = \rho_{00}\left(r(z) + \tilde{\rho}(x,y,z,t)\right),\\
&\operatorname{div}\mathbf{u} = 0.
\end{aligned} \tag{2.3}$$

Here, $\tilde{\rho}(x,z,t)$ is the density perturbation associated with the propagation of a periodic flow, and $r(z)$ is a function of the initial undisturbed density distribution over the fluid depth. For a wide range of problems, equilibrium distribution can be assumed exponential $r(z)=\exp(-z_\Lambda)$ or linear $r(z)=(1-z_\Lambda)$. In this case, $z_\Lambda = z/\Lambda$ is a dimensionless vertical coordinate that determines the depth in relation to stratification scale $\Lambda = \left|d\ln\rho(z)/dz\right|^{-1}$. Scale transformation enables a transition from system in Eq (2.3) with an arbitrary smooth density profile and buoyancy frequency to a system of internal wave equations with constant coefficients [36]. In this work, an exponential density distribution will be used.

Equation (2.3) is supplemented with initial and boundary conditions depending on the type of flows under study and the geometry considered. For capillary-gravity disturbances of the free surface, the boundary conditions are discussed below.

2.3. Perturbations of fluid free surface

When considering the oscillations of fluid free surface, it is important to take into account the change in its geometry. This change is connected with gravity and the impact of fluid surface tension. To describe of these factors correctly, it is necessary to write physically substantiated boundary conditions on a free surface that regards kinematic and dynamic relations on the free surface. The kinematic relation states the equality of fluid velocity and the velocity of surface movement over time [17,78]:

$$\frac{DF}{Dt} = \frac{\partial F}{\partial t} + (\mathbf{u}\cdot\nabla)F = 0. \tag{2.4}$$

Dynamic relation in the absence of an external dynamic load on a free surface is written as [17,78]:

$$n_j \sigma^{ij} = \sigma \nabla_j n^j. \tag{2.5}$$

Here, $\mathbf{n}$ is a single vector of the external normal to the free surface, and σ is the coefficient of surface tension. It is also necessary to include natural conditions for the attenuation of surface periodic motion with depth [17,78]:

$$\mathbf{u}\big|_{z\to-\infty} \to 0. \tag{2.6}$$

For a solenoid field of velocities in a two-dimensional formulation, it is possible to represent the velocity components employing a single scalar stream function ψ:

$$\mathbf{u} = \left(\frac{\partial\psi}{\partial z}, -\frac{\partial\psi}{\partial x}\right). \tag{2.7}$$

The mathematical formulation of a problem in Eqs (2.3)–(2.6), considering Eq (2.7) for an exponentially stratified viscous incompressible fluid, is simplified:

$$z<\zeta:\begin{cases}\rho\left(\partial_{zt}\psi-\partial_x\psi\partial_{zz}\psi+\partial_z\psi\partial_{xz}\psi\right)=-\nu\rho\partial_z\Delta\psi-\partial_x P,\\ \rho\left(-\partial_{xt}\psi+\partial_x\psi\partial_{xz}\psi-\partial_z\psi\partial_{xx}\psi\right)=\nu\rho\partial_x\Delta\psi-\partial_z P+\rho g,\\ \partial_t\rho+\partial_x\rho\partial_z\psi-\partial_z\rho\partial_x\psi=0,\\ \rho=\rho_{00}\left(\exp\left(-z_\Lambda\right)+\tilde{\rho}\left(x,y,z,t\right)\right),\end{cases} \tag{2.8}$$

$$z=\zeta:\begin{cases}\partial_t(z-\zeta)-\partial_z\psi\partial_x\zeta-\partial_x\psi+\partial_x\psi\partial_x\zeta=0,\\ \dfrac{1}{1+\left(\partial_x\zeta\right)^2}\left(\left(\partial_x\zeta\right)^2\partial_{xx}\psi-2\partial_x\zeta\partial_{xz}\psi+\partial_{zz}\psi\right)-\dfrac{1}{1+\left(\partial_x\zeta\right)^2}\left(\left(\partial_x\zeta\right)^2\partial_{zz}\psi+2\partial_x\zeta\partial_{xz}\psi+\partial_{xx}\psi\right)=0,\\ P-P_0+\dfrac{\sigma\partial_{xx}\zeta}{\left(1+\left(\partial_x\zeta\right)^2\right)^{3/2}}-\dfrac{2\rho\nu}{1+\left(\partial_x\zeta\right)^2}\left[\left(\left(\partial_x\zeta\right)^2-1\right)\partial_{xz}\psi+\partial_x\zeta\left(\partial_{xx}\psi-\partial_{zz}\psi\right)\right]=0,\end{cases} \tag{2.9}$$

$$z=\to-\infty:\qquad \left(\frac{\partial\psi}{\partial z},-\frac{\partial\psi}{\partial x}\right)\to\left(0,0\right). \tag{2.10}$$

The fluid pressure can be described as the sum of atmospheric P_0, hydrostatic, and periodic $\tilde{P}\left(x,z,t\right)$ pressure perturbations.

$$P=P_0+\int_z^\zeta g\rho\left(x,\xi,t\right)d\xi+\tilde{P}(x,z,t). \tag{2.11}$$

In the problem under consideration, there is a set of natural problem scales, with large and small values.

The time scales in the incompressible fluid model are determined by the buoyancy frequency N, which takes values $N\sim 1\ldots 10^{-5},\ \mathrm{s}^{-1}$ in laboratory and natural conditions.

The spatial parameters of the problem are defined by scale of stratification, taking the values Λ, combined Rayleigh scale $\delta_N^{g\nu}=\left(g\nu\right)^{1/3}N^{-1}$, microscale $\delta_N^{\nu}=\sqrt{\nu/N}$ (the values are given in Table 1), Stokes viscous wave scale $\delta_\omega^{g\nu}=\left(g\nu\right)^{1/3}\omega^{-1}$, and microscale $\delta_\omega^{\nu}=\sqrt{\nu/\omega}$.

When considering infinitesimal perturbations with a wavelength that significantly exceeds its amplitude $\lambda\gg A$, it is acceptable to represent the required functions as an expansion into infinite series in terms of a small parameter $\varepsilon=A/\lambda$, which makes sense of the wave steepness:

$$f=f_0+\varepsilon f_1+\varepsilon^2 f_2+\ldots \tag{2.12}$$

Substituting the type of unknown Eq (2.12) into Eq (2.8) and taking into Eq (2.11), we can obtain the problem decomposed into the orders of magnitude based on the amplitude of periodic perturbations.

Before linearizing the problem, we need to remove the boundary conditions on the equilibrium surface $z = 0$ following the procedure described in detail in [79,80] and the justification given in [81]. After selecting the terms of the first order of smallness, we receive the problem in a linear approximation [75,76]:

$$z < 0: \begin{cases} \rho_{00} g \partial_x \zeta + \rho_{00} g \int_z^0 \partial_x \tilde{\rho}(x, \xi, t)\, d\xi + \rho_{00}\, e^{-z_\Lambda}\, \partial_{zt}\psi - \nu \rho_{00}\, e^{-z_\Lambda}\, \partial_z \Delta\psi + \partial_x \tilde{P} = 0, \\ -\rho_{00}\, e^{-z_\Lambda}\, \partial_{xt}\psi + \nu \rho_{00}\, e^{-z_\Lambda}\, \partial_x \Delta\psi + \partial_z \tilde{P} = 0, \\ \rho_{00} g \partial_t \tilde{\rho} + \rho_{00} N^2\, e^{-z_\Lambda}\, \partial_x \psi = 0, \end{cases} \tag{2.13}$$

$$z = 0: \begin{cases} \partial_t \zeta + \partial_x \psi = 0, \\ \partial_{zz}\psi - \partial_{xx}\psi = 0, \\ \tilde{P} + \sigma \partial_{xx}\zeta + 2\rho\nu \partial_{xz}\psi = 0, \end{cases} \tag{2.14}$$

$$z = \to -\infty: \qquad \left(\frac{\partial \psi}{\partial z}, -\frac{\partial \psi}{\partial x} \right) \to (0, 0). \tag{2.15}$$

Here, $N^2 = g/\Lambda$ is the square of the buoyancy frequency in an incompressible fluid, which determines the oscillation frequency of a body with neutral buoyancy located at level z. In exponentially stratified fluids, the buoyancy frequency is a constant value $N = \text{const}$. In general, the buoyancy frequency changes with depth and is the function of the vertical coordinate $N = N(z)$. For a wide range of problems, if the scales of phenomena are not much larger than the scale of medium buoyancy Λ, the buoyancy frequency can be considered constant, and the medium can be assumed uniformly stratified.

In Eqs (2.13)–(2.15) and subsequent ones, index "1" is omitted. Index 1 denotes the corresponding order of magnitude for compactness. This is because in the future, only values of the first order of smallness in wave amplitude will be used, unless otherwise stated.

We use the immersion of the problem into the algebra of complex numbers and look for a solution to Eqs (2.13)–(2.15) in the form of periodic harmonic functions:

$$\begin{pmatrix} \zeta \\ \psi \\ \tilde{P} \\ \tilde{\rho} \end{pmatrix} = \begin{pmatrix} A \\ \Psi_m \exp(k_z z) \\ P_m \exp(k_z z) \\ R_m \exp(k_z z) \end{pmatrix} \exp(i k_x x - i\omega t) + C.C. \tag{2.16}$$

Here, A, Ψ_m, P_m, R_m are amplitude multipliers, ω stands for the frequency of periodic motion, $\mathbf{k} = (k_x, k_z)$ is the wave vector, and the symbol $C.C.$ denotes complex conjugate summands.

The frequency of periodic motion, which is a value that determines the amount of energy, remains actual and positively determined; $\omega > 0$. The components of the wave vector that define the periodic motion and the spatial attenuation of the flow components can be complex $k_{x,z} \in \mathbb{C}$, where $\mathbb{C}$ stands for the set of complex numbers.

Using cross-differentiation, we can reduce the system in Eq (2.13) to an equation involving a single scalar stream function ψ:

$$\partial_{tt}\Delta\psi - \nu\partial_t\Delta\Delta\psi + \frac{\nu}{\Lambda}\partial_{zt}\Delta\psi - \frac{1}{\Lambda}\partial_{ztt}\psi + N^2\partial_{xx}\psi = 0. \tag{2.17}$$

By substituting the form of Eq (2.16) into Eq (2.17), we can obtain the equation of motion in spectral form, which connects the vertical components of the wave vector k_z with the horizontal k_x, frequency, and other parameters of the problem.

$$\omega\left(k_x^2 - k_z^2\right)\left(i\nu\left(k_x^2 - k_z^2\right) + \omega\right) + \frac{\omega k_z}{\Lambda}\left(i\nu\left(k_x^2 - k_z^2\right) + \omega\right) - N^2 k_x^2 = 0. \tag{2.18}$$

The vertical component of the wave vector k_z stands out naturally due to the stratification along the axis Oz. Therefore, we seek the solution to Eq (2.18) for function $k_z = k_z\left(k_x, \omega\right)$. It is worth noting that Eq (2.18) is of the fourth order with respect to required value k_z, and thus has four roots that can be found precisely.

$$\begin{aligned} &k_{z1} = \frac{1}{4\Lambda} + \frac{A}{2} - \frac{1}{2}\sqrt{G + \frac{B}{4A}},\ k_{z2} = \frac{1}{4\Lambda} + \frac{A}{2} + \frac{1}{2}\sqrt{G + \frac{B}{4A}}, \\ &k_{z3} \equiv k_{l1} = \frac{1}{4\Lambda} - \frac{A}{2} - \frac{1}{2}\sqrt{G - \frac{B}{4A}},\ k_{z4} \equiv k_{l2} = \frac{1}{4\Lambda} - \frac{A}{2} + \frac{1}{2}\sqrt{G - \frac{B}{4A}}, \end{aligned} \tag{2.19}$$

$$\begin{aligned} &A = \sqrt{\theta - \frac{2\kappa}{3} + \frac{1}{4\Lambda^2} + \upsilon},\ B = \frac{1}{\Lambda}\left(\frac{1}{\Lambda^2} - 4\kappa - \frac{8\Theta}{\nu}\right),\ G = \frac{1}{2\Lambda^2} - \theta - \frac{4\kappa}{3} - \upsilon, \\ &\theta = \frac{\left(i + \sqrt{3}\right)\beta^{1/3}}{6 \cdot 2^{1/3}\Lambda\nu\omega},\ \upsilon = \frac{2^{1/3}\left(i - \sqrt{3}\right)\alpha}{6\beta^{1/3}\Lambda\nu\omega},\ \Theta = k_x^2\nu - i\omega,\ \kappa = -k_x^2 - \frac{\Theta}{\nu}, \\ &\alpha = \omega\left(\Lambda^2\left(\omega^3 - 12ik_x^2N^2\nu\right) - \Theta\nu\omega\left(3 + 16k_x^2\Lambda^2\right)\right),\ \beta = \frac{iD}{\Lambda\omega^2} + i\sqrt{4\alpha^3 + \Lambda^2 D^2\omega^4}, \\ &D = 9ik_x^2N^2\nu^2\left(3 - 8\kappa\Lambda^2\right) + 2\kappa\nu\omega\left(\Theta\nu\left(9 + 32k_x^2\Lambda^2\right) + \Lambda^2\omega^2\right). \end{aligned}$$

In Eq (2.19), a reinterpretation was made for the roots k_{z3}, k_{z4} because these roots correspond to singular solutions of Eq (2.18). The procedure determining the type of solution (i.e., regular or singular) is described in detail in [76]. Regular components of the solution correspond to large-scale wave perturbations, while singular components correspond to ligaments that characterize the fine structure of a heterogeneous medium.

We will perform the limiting transitions for the wave and ligament roots in Eq (2.19) to the model of a homogeneous weakly viscous fluid. To do this, it is necessary to compute the limiting expressions as $\Lambda \to +\infty$ and retain only the leading-order terms with respect to the kinematic viscosity. Carefully carrying out this procedure yields the following well-known relations for waves and ligaments in a homogeneous fluid:

$$k_{z1} \to -k_x,\ k_{z2} \to k_x,\ k_{l1} \to -\sqrt{k_x^2 - \frac{i\omega}{\nu}},\ k_{l2} \to \sqrt{k_x^2 - \frac{i\omega}{\nu}}.$$

When performing the limiting transitions to a homogeneous fluid, the ligament solutions disappear.

The difference between wave roots and ligament roots can be formalized by noting the relationship between the imaginary and real parts of the regular and singular solutions. For waves, a large difference between the magnitudes of the imaginary and real parts of the solution is characteristic, while ligaments exhibit imaginary and real components that are close in magnitude:

$$\left|\operatorname{Im}(k_z)\right| \ll \left|\operatorname{Re}(k_z)\right|,\ \left|\operatorname{Im}(k_l)\right| \sim \left|\operatorname{Re}(k_l)\right|.$$

The expansion of the problem space in the process of immersion in the algebra of complex numbers leads to the emergence of additional solutions and methods of their construction. To select the correct solutions, it is necessary to impose conditions on the physical feasibility of roots. For surface periodic flows, the condition for natural attenuation of motion with depth in Eq (2.15) is chosen as such a condition. For the components of the wave vector, this condition can be written as:

$$\operatorname{Re}(k_z) > 0. \tag{2.20}$$

Taking into account Eq (2.20), only two solutions from Eq (2.19) are physically realizable, i.e., one regular wave solution and one singular ligament solution.

Considering all the flow components, the type of solution for the stream function changes:

$$\psi = \left(\Psi_m^w \exp(k_z z) + \Psi_m^l \exp(k_l z)\right)\exp(ik_x x - i\omega t) + C.C. \tag{2.21}$$

Here, Ψ_m^w, Ψ_m^l are the amplitude multipliers for the wave (regular) and ligament (singular) components of the stream function:

Taking into account Eq (2.21) and the condition for compatibility of the basic Eq (2.13) and boundary conditions in Eq (2.14), we can obtain a spectral dispersion relation that connects the horizontal component of the wave vector with frequency and other parameters of the problem [76]:

$$\begin{aligned}&\left(k_x^2 + k_z^2\right)\left(k_l\omega^2 - gk_x^2 - \gamma k_x^4 + i\omega\nu k_l\left(3k_x^2 - k_l^2\right)\right)\\ &-\left(k_x^2 + k_l^2\right)\left(k_z\omega^2 - gk_x^2 - \gamma k_x^4 + i\omega\nu k_z\left(3k_x^2 - k_z^2\right)\right) = 0.\end{aligned} \tag{2.22}$$

Here, $\gamma = \sigma/\rho_{00}$ is the coefficient of fluid surface tension, which is normalized for the equilibrium value of density at zero. An accurate solution to a high-degree algebraic Eq (2.22) is not found analytically; asymptotic or numerical methods have to be applied for its construction [76]. To ensure the compatibility of boundary conditions with the basic equations, we use complete solutions to the spectral equation of motion in Eq (2.19).

In this study, we employ the procedure of numerical calculation of dispersion equation roots in Eq (2.22) using exact solutions for the dispersion relations of waves and ligaments Eq (2.19) in construction and analysis of solutions. When solving Eq (2.22), the roots that correspond to the perturbation propagation in the positive and negative directions of the horizontal axis Ox emerge. Here and further, we consider only perturbations propagating in the positive direction. Mathematically, this limitation can be expressed as:

$$\operatorname{Im}\left(k_x\right) > 0. \tag{2.23}$$

To consider negatively directed perturbations, it is necessary to choose solutions with the opposite sign. The solution of the dispersion equation in Eq (2.22) is sought, taking into account the limitations in Eqs (2.20) and (2.23) for waves and ligaments determined by the relations in Eq (2.19). To write the dispersion equation explicitly, we choose expressions for the wave component k_z and the ligament component k_l from the expressions in Eq (2.19), satisfying the relation in Eq (2.20). Thus, when we substitute the chosen expressions into Eq (2.22), Eq (2.23) is satisfied automatically. For this purpose, we develop a special procedure for solution selection, the results of which are presented below. In constructing numerical solutions, approaches based on the Newton–Raphson algorithm or homotopy with linear homotopy are employed. The approach is chosen depending on the system of equations being solved.

2.4. Internal waves

To describe internal waves in the thickness of a stratified fluid, harmonic functions of $f(x,z) \propto A\exp\left(ik_x x + ik_z z - i\omega t\right)$ type are used instead of form Eq (2.16). In this case, when we substitute the type of solution into the basic equations of motion, the spectral representation of the equations of motion becomes:

$$\omega\left(k_x^2+k_z^2\right)\left(i\nu\left(k_x^2+k_z^2\right)+\omega\right)+\frac{i\omega k_z}{\Lambda}\left(i\nu\left(k_x^2+k_z^2\right)+\omega\right)-N^2k_x^2=0. \tag{2.24}$$

The solutions to the spectral equation of motion in Eq (2.24), which describes internal gravitational waves, also include regular and singular roots. These roots have the following form:

$$\begin{gathered}
k_{z1}^i=\frac{A^i}{2}-\frac{i}{4\Lambda}-\frac{1}{2}\sqrt{G^i+\frac{B^i}{4A^i}},\ k_{z2}^i=\frac{A^i}{2}-\frac{i}{4\Lambda}+\frac{1}{2}\sqrt{G^i+\frac{B^i}{4A^i}},\\
k_{z3}^i\equiv k_{l1}^i=-\frac{A^i}{2}-\frac{i}{4\Lambda}-\frac{1}{2}\sqrt{G^i-\frac{B^i}{4A^i}},\ k_{z4}^i\equiv k_{l2}^i=-\frac{A^i}{2}-\frac{i}{4\Lambda}+\frac{1}{2}\sqrt{G^i-\frac{B^i}{4A^i}},
\end{gathered} \tag{2.25}$$

$$A^i = \sqrt{\theta^i + \frac{2\kappa}{3} - \frac{1}{4\Lambda^2} + \upsilon^i},\ B^i = \frac{i}{\Lambda}\left(\frac{1}{\Lambda^2} - 4\kappa - \frac{8\Theta}{\nu}\right),\ G^i = -\frac{1}{2\Lambda^2} - \theta^i + \frac{4\kappa}{3} - \upsilon^i,$$

$$\theta^i = \frac{\left(i+\sqrt{3}\right)\beta^{i1/3}}{6\cdot 2^{1/3}\Lambda\nu\omega},\ \upsilon^i = \frac{2^{1/3}\left(i-\sqrt{3}\right)\alpha}{6\beta^{i1/3}\Lambda\nu\omega},\ \Theta = k_x^2\nu - i\omega, \kappa = -k_x^2 - \frac{\Theta}{\nu},$$

$$\alpha = \omega\left(\Lambda^2\left(\omega^3 - 12ik_x^2N^2\nu\right) - \Theta\nu\omega\left(3 + 16k_x^2\Lambda^2\right)\right),\ \beta^i = -\frac{iD}{\Lambda\omega^2} + i\sqrt{4\alpha^3 + \Lambda^2D^2\omega^4},$$

$$D = 9ik_x^2N^2\nu^2\left(3 - 8\kappa\Lambda^2\right) + 2\kappa\nu\omega\left(\Theta\nu\left(9 + 32k_x^2\Lambda^2\right) + \Lambda^2\omega^2\right).$$

Equation (2.25) characterizes regular wave solutions for internal gravitational waves and the ligament solutions, which accompany the waves and are denoted by the subscript "l". The presence of a free surface causes dispersion for internal waves and, where the dispersion equation in Eq (2.22) can be simplified, occurs to be justified. Capillarity has no significant impact on the propagation of internal waves in a liquid thickness, and terms related to surface tension can be ignored in the dispersion equation.

$$\left(k_x^2 + k_z^2\right)\left(k_l\omega^2 - gk_x^2 + i\omega\nu k_l\left(3k_x^2 - k_l^2\right)\right) - \left(k_x^2 + k_l^2\right)\left(k_z\omega^2 - gk_x^2 + i\omega\nu k_z\left(3k_x^2 - k_z^2\right)\right) = 0. \tag{2.26}$$

Substituting Eq (2.25), chosen in accordance with the condition of physical feasibility, into Eq (2.26), we obtain an explicit dispersion relation. This relation turns out to be rather complicated. The accurate analytical solution to the resulting equation is difficult, so we can use numerical methods to solve it.

2.5. Boussinesq approximation

In the research of stratified fluids, the Boussinesq approximation is often employed to simplify mathematical calculations [36, 82, 83]. In this approximation, the density is regarded to be variable only for large summands and it is assumed to be constant and equal to its equilibrium value at zero level ρ_{00} for the rest of the terms. The Boussinesq approximation enables us to rewrite the mathematical formulation of the linearized problem in Eqs (2.13)–(2.15) for viscous incompressible fluid, as follows [76]:

$$z < 0: \begin{cases} \rho_{00}g\partial_x\zeta + \rho_{00}g\int_z^0 \partial_x\tilde{\rho}(x,\xi,t)\,d\xi + \rho_{00}\partial_{tz}\psi - \rho_{00}\nu\partial_z\Delta\psi + \partial_x\tilde{P} = 0, \\ -\rho_{00}\partial_{tx}\psi + \rho_{00}\nu\partial_x\Delta\psi + \partial_z\tilde{P} = 0, \\ \partial_t\tilde{\rho} - \dfrac{\rho_{00}}{\Lambda}\exp\left(-z_\Lambda\right)\partial_x\psi = 0, \end{cases} \tag{2.27}$$

$$z = 0: \begin{cases} \partial_t\zeta + \partial_x\psi = 0, \\ \partial_{zz}\psi - \partial_{xx}\psi = 0, \\ \tilde{P} + \sigma\partial_{xx}\zeta + 2\rho\nu\partial_{xz}\psi = 0, \end{cases} \tag{2.28}$$

$$z = \to -\infty: \qquad \left(\frac{\partial\psi}{\partial z}, -\frac{\partial\psi}{\partial x}\right) \to (0,0). \tag{2.29}$$

By implementing the procedure of reducing system in Eq (2.27) to an equation in terms of a single scalar stream function, which is analogous to the one performed in the previous paragraph, we get the expression:

$$\partial_{tt}\Delta\psi - \nu\partial_t\Delta\Delta\psi + N^2\exp(-z_\Lambda)\partial_{xx}\psi = 0.$$

Utilizing the harmonic type of solution in Eq (2.16), we can obtain the equation of motion in a spectral form, which associates the components of a complex wave vector with a positive real frequency in the Boussinesq approximation:

$$\omega\left(k_x^2 - k_z^2\right)\left(i\nu\left(k_x^2 - k_z^2\right) + \omega\right) - N^2 k_x^2 \exp(-z_\Lambda) = 0. \tag{2.30}$$

Comparing Eq (2.30) to Eq (2.18), several characteristic peculiarities can be noticed. First, the structure of the dispersion equation is different. In the complete formulation, additional summands appear.

$$\frac{\omega k_z}{\Lambda}\left(i\nu\left(k_x^2 - k_z^2\right) + \omega\right).$$

They do not change the order of the equation but complicate the analytical solution and affect the final expressions for the wave and ligament roots. A detailed analysis of the impact on the characteristics of the solution is provided below.

Second, there is no dependence of roots of the equation of motion in a spectral form on the vertical coordinate z in the complete formulation. However, it emerges in the model with the Boussinesq approximation. Since the problem concerns surface oscillations and the stratification scales usually have large values, ranging from hundreds of meters to tens of kilometers depending on the conditions, the exponential parameter z_Λ in Eq (2.30) occurs to be small. Therefore, a series expansion in a small parameter is acceptable.

$$\exp(-z_\Lambda) = 1 - z_\Lambda + O\left(z_\Lambda^2\right) \approx 1. \tag{2.31}$$

The series Eq (2.31) is used in the following constructions. Equation (2.30) is discussed in detail in [76]. The problem also identifies two regular wave roots, k_z, and two singular ligament roots, k_z, which are found:

$$k_{z1,2} = \pm\sqrt{k_x^2 - \frac{i\omega}{2\nu} - \frac{(1-i)\sqrt{4k_x^2\nu\omega N^2\exp(-z_\Lambda) - i\omega^4}}{2\sqrt{2}\nu\omega}},$$

$$k_{z3,4} = k_{l1,2} = \pm\sqrt{k_x^2 - \frac{i\omega}{2\nu} + \frac{(1-i)\sqrt{4k_x^2\nu\omega N^2\exp(-z_\Lambda) - i\omega^4}}{2\sqrt{2}\nu\omega}}. \tag{2.32}$$

Considering the approximate decomposition given in Eq (2.31), we can derive expressions for the roots:

$$k_{z1,2} = \pm\sqrt{K_- - K_N},\ k_{l1,2} = \pm\sqrt{K_- + K_N},$$
$$K_- = k_x^2 - \frac{i\omega}{2\nu},\ K_N = \frac{1-i}{\sqrt{2\nu\omega}}\sqrt{k_x^2 N^2 - \frac{i\omega^3}{4\nu}}. \tag{2.33}$$

The dispersion relation links the horizontal component of the wave vector with frequency and arises from the compatibility condition of the boundary Eqs (2.28) and (2.29), as well as Eq (2.27). This relation does not formally differ from Eq (2.22) obtained in the complete formulation. However, it is worth noting that differences appear explicitly when substituting the Eq (2.33), due to the difference in the wave and ligament components in the complete formulation and in the Boussinesq approximation.

Explicitly, the dispersion equation is written as follows:

$$\begin{gathered}(K_{2-} - K_N)\left[\omega^2\sqrt{K_- + K_N} - gk_x^2 - \gamma k_x^4 + i\omega\nu\sqrt{K_- + K_N}\left(K_{2+} - K_N\right)\right] \\ -(K_{2-} + K_N)\left[\omega^2\sqrt{K_- - K_N} - gk_x^2 - \gamma k_x^4 + i\omega\nu\sqrt{K_- - K_N}\left(K_{2+} + K_N\right)\right] = 0, \\ K_{2-} = 2k_x^2 - \frac{i\omega}{2\nu},\ K_{2+} = 2k_x^2 + \frac{i\omega}{2\nu}.\end{gathered} \tag{2.34}$$

In this paper, we solve Eq (2.34) using numerical methods with a specially designed procedure by analogy to complete formulation of the problem. Furthermore, the solutions to Eq (2.22) and the flow Eq (2.33) are limited as Eqs (2.20) and (2.23).

Internal gravitational waves in the Boussinesq approximation were analyzed in detail in [36]. It is known that the spectral representation of the equation of motion for internal gravitational waves is written as follows [36]:

$$ik_x^4\omega\nu + k_z^2\omega\left(ik_z^2\nu + \omega\right) + k_x^2\left(\omega\left(2i\nu k_z^2 + \omega\right) - N^2\right) = 0. \tag{2.35}$$

The solution to Eq (2.35) can be found by standard methods. It contains singular and regular roots (as in the case with surface waves):

$$k_{z1,2} = \pm i\sqrt{K_+ - K_N},\quad k_{z3,4} = k_{l1,2} = \pm i\sqrt{K_- + K_N},$$
$$K_+ = k_x^2 + \frac{i\omega}{2\nu}. \tag{2.36}$$

By analogy with the surface periodic flows, we reinterpret the singular solutions k_l that define the fine-structured ligament components in Eq (2.36).

2.6. Ideal fluid approximation

When considering gravitational surface waves, the viscosity of the liquid is often neglected at the stage of problem formulation. Mathematical formulation is extremely reduced in this case. In an ideal fluid model, the momentum transfer equation is replaced by the Euler equation, and the boundary conditions are considerably simplified. This simplification is associated with the change in the type of stress tensor. There are no summands determined by the viscous stress tensor in an ideal liquid.

The mathematical formulation of the problem in the model of an ideal incompressible exponentially stratified fluid is written as follows [17,75]:

$$z<\zeta:\begin{cases}\rho\left(\partial_{zt}\psi-\partial_x\psi\partial_{zz}\psi+\partial_z\psi\partial_{xz}\psi\right)=-\partial_x P,\\ \rho\left(-\partial_{xt}\psi+\partial_x\psi\partial_{xz}\psi-\partial_z\psi\partial_{xx}\psi\right)=-\partial_z P+\rho g,\\ \partial_t\rho+\partial_x\rho\partial_z\psi-\partial_z\rho\partial_x\psi=0,\\ \rho=\rho_{00}\left(\exp\left(-z_\Lambda\right)+\tilde{\rho}\left(x,y,z,t\right)\right),\end{cases} \tag{2.37}$$

$$z=\zeta:\begin{cases}\partial_t(z-\zeta)-\partial_z\psi\partial_x\zeta-\partial_x\psi+\partial_x\psi\partial_x\zeta=0,\\ P-P_0+\dfrac{\sigma\partial_{xx}\zeta}{\left(1+\left(\partial_x\zeta\right)^2\right)^{3/2}}=0,\end{cases} \tag{2.38}$$

$$z=\rightarrow-\infty:\qquad \left(\frac{\partial\psi}{\partial z},-\frac{\partial\psi}{\partial x}\right)\rightarrow\left(0,0\right). \tag{2.39}$$

After the linearization procedure and the removal of boundary Eq (2.38) on the equilibrium surface, the mathematical Eqs (2.37)–(2.39) can be rewritten as:

$$z<0:\begin{cases}\rho_{00}g\partial_x\zeta+\rho_{00}g\int_z^0\partial_x\tilde{\rho}\left(x,\xi,t\right)d\xi+\rho_{00}\,\mathrm{e}^{-z_\Lambda}\,\partial_{zt}\psi+\partial_x\tilde{P}=0,\\ -\rho_{00}\,\mathrm{e}^{-z_\Lambda}\,\partial_{xt}\psi+\partial_z\tilde{P}=0,\\ \rho_{00}g\partial_t\tilde{\rho}+\rho_{00}N^2\,\mathrm{e}^{-z_\Lambda}\,\partial_x\psi=0,\end{cases} \tag{2.40}$$

$$z=0:\begin{cases}\partial_t\zeta+\partial_x\psi=0,\\ \tilde{P}+\sigma\partial_{xx}\zeta=0,\end{cases} \tag{2.41}$$

$$z=\rightarrow-\infty:\qquad \left(\frac{\partial\psi}{\partial z},-\frac{\partial\psi}{\partial x}\right)\rightarrow\left(0,0\right). \tag{2.42}$$

Using cross-differentiation, system in Eq (2.40) results in an equation regarding a single scalar stream function ψ:

$$\partial_{tt}\Delta\psi-\frac{1}{\Lambda}\partial_{ztt}\psi+N^2\partial_{xx}\psi=0. \tag{2.43}$$

Substituting the solution type in Eq (2.16) into Eq (2.43), we obtain the spectral form of the equation of motion in the ideal fluid model:

$$\omega^2\left(k_x^2-k_z^2\right)+\frac{\omega^2 k_z}{\Lambda}-N^2k_x^2=0. \tag{2.44}$$

The spectral form of the equation of motion is of the second order with respect to the vertical component of the wave vector k_z, and has corresponding analytical solutions:

$$k_{z1}=\frac{\omega^2-\sqrt{\omega^4+4k_x^2\Lambda^2\omega^2\left(\omega^2-N^2\right)}}{2\Lambda\omega^2},$$
$$k_{z2}=\frac{\omega^2+\sqrt{\omega^4+4k_x^2\Lambda^2\omega^2\left(\omega^2-N^2\right)}}{2\Lambda\omega^2}. \tag{2.45}$$

Considering the compatibility of Eq (2.40) and boundary Eq (2.41), we get the dispersion equation for an ideal fluid in a spectral registration.

$$gk_x^2-\omega^2k_z+\gamma k_x^4=0. \tag{2.46}$$

Equation (2.46) is solved accurately, and the solutions should be limited, similar to those in Eqs (2.20) and (2.23). Moreover, Eq (2.20) is satisfied only by the root k_{z2} in Eq (2.45). By substituting it into the Eq (2.46):

$$k_x^2=\frac{\mu^2-\omega^4}{4\Lambda^2\omega^2\left(\omega^2-N^2\right)}, \tag{2.47}$$

we obtain the equation with respect to an auxiliary variable μ:

$$g\frac{\mu^2-\omega^4}{4\Lambda^2\omega^2\left(\omega^2-N^2\right)}-\omega^2\frac{\omega^2+\mu}{2\Lambda\omega^2}+\gamma\left(\frac{\mu^2-\omega^4}{4\Lambda^2\omega^2\left(\omega^2-N^2\right)}\right)^2=0. \tag{2.48}$$

The solution to Eq (2.48) is found by standard methods:

$$\mu_1=-\omega^2, \qquad \mu_2=\frac{1}{3}\left[\omega^2+\frac{2^{1/3}\theta}{\gamma}+\frac{2\cdot 2^{1/3}\left(\gamma\omega^4-3g\Lambda^2\omega^2\left(\omega^2-N^2\right)\right)}{\theta}\right],$$
$$\mu_{3,4}=\frac{1}{6}\left[2\omega^2\pm\frac{2^{2/3}\theta i\left(\sqrt{3}\pm i\right)}{\gamma}\mp\frac{2\cdot 2^{1/3} i\left(\sqrt{3}\mp i\right)\left(\gamma\omega^4-3g\Lambda^2\omega^2\left(\omega^2-N^2\right)\right)}{\theta}\right],$$
$$\theta=\left(\gamma^2\omega^4\left(27N^4\Lambda^3-2\gamma\omega^2-54N^2\Lambda^3\omega^2+27\Lambda^3\omega^4+9g\Lambda^2\left(\omega^2-N^2\right)\right)\right.$$
$$\left.+3\sqrt{3}\gamma^{3/2}\Lambda^{3/2}\omega^3\left(\omega^2-N^2\right)\times\sqrt{4g^3\Lambda^3\left(\omega^2-N^2\right)-g^2\gamma\Lambda\omega^2+18g\gamma\Lambda^2\omega^2\left(\omega^2-N^2\right)-\gamma\omega^2\left(4\gamma\omega^2-27N^4\Lambda^3+54N^2\Lambda^3\omega^2-27\Lambda^3\omega^4\right)}\right)^{1/3}. \tag{2.49}$$

Substituting Eq (2.49) into Eq (2.47) and applying Eq (2.23), we obtain an accurate solution to the dispersion Eq (2.46). This precise solution to the problem in the ideal fluid model can be compared to the solutions obtained for the wave component in the viscous fluid model.

2.7. Ideal fluid model in the Boussinesq approximation

In the ideal fluid model with the application of the Boussinesq approximation, the mathematical formulation of a linearized problem can be written as follows [17,75]:

$$z<0:\begin{cases}\rho_{00}g\partial_x\zeta+\rho_{00}g\int_z^{\zeta}\partial_x\tilde{\rho}(x,\xi,t)\,d\xi+\rho_{00}\partial_{tz}\psi+\partial_x\tilde{P}=0,\\ -\rho_{00}\partial_{tx}\psi+\partial_z\tilde{P}=0,\\ \partial_t\tilde{\rho}-\dfrac{\rho_{00}}{\Lambda}\exp\left(-z_\Lambda\right)\partial_x\psi=0,\end{cases} \tag{2.50}$$

$$z=0:\begin{cases}\partial_t\zeta+\partial_x\psi=0,\\ \tilde{P}+\sigma\partial_{xx}\zeta=0,\end{cases} \tag{2.51}$$

$$z=\to-\infty: \qquad \left(\frac{\partial\psi}{\partial z},-\frac{\partial\psi}{\partial x}\right)\to(0,0). \tag{2.52}$$

When system in Eq (2.50) is led to an equation with respect to a single scalar function, which is the stream function, we get:

$$\partial_{tt}\Delta\psi+N^2\exp\left(-z_\Lambda\right)\partial_{xx}\psi=0. \tag{2.53}$$

From Eq (2.53) (using the type of solution in Eq (2.16)) we can obtain the dispersion equation.

$$\omega^2\left(k_x^2-k_z^2\right)-N^2\exp\left(-z_\Lambda\right)k_x^2=0. \tag{2.54}$$

The obvious difference of Eq (2.54) from Eqs (2.18) and (2.30) lies in its order. In an ideal liquid model, the dispersion equation is of the second order. Equation (2.44) emerges in an ideal fluid model that does not employ the Boussinesq approximation. The distinction is in two aspects. First, there is no additional summand $\omega^2 k_z/\Lambda$, and second, the solution depends on the vertical coordinate z, similar to the viscous fluid model in the Boussinesq approximation. Solutions to Eq (2.54) can be found and expressed as follows:

$$k_z = \pm\sqrt{k_x^2\left(1-N_\omega^2 \exp\left(-z_\Lambda\right)\right)},\ N_\omega = N/\omega. \tag{2.55}$$

A detailed analysis shows that roots in Eq (2.55) correspond to regular solutions of Eq (2.30) [75]. Thus, when we switch to the inviscid liquid model, neglecting low viscosity at the stage of formulation rather than at the stage of considering solutions, the system of equations and the composition of the periodic surface flow change qualitatively. In an ideal liquid, only wave components exist. It is not possible to obtain fine-structured ligament components in this model.

For an ideal fluid in the Boussinesq approximation, the considerations regarding the exponential Eq (2.31) and the use of approximate roots for constructing solutions also hold true.

$$k_z = \pm\sqrt{k_x^2\left(1-N_\omega^2\right)}.$$

Taking into account the compatibility condition of boundary Eqs (2.50) and (2.51) and the basic equations, we obtain a dispersion relation that is analogous in form to Eq (2.46). However, there is a difference in the root k_z that is substituted into the dispersion equation.

When we substitute the explicit form of the solution for the vertical component of the wave vector k_z, the dispersion equation becomes:

$$k_x^3 + \frac{g}{\gamma}k_x - \frac{\omega^2\sqrt{\left(1-N_\omega^2\right)}}{\gamma} = 0. \tag{2.56}$$

The solutions to Eq (2.56) can be found by standard methods for solving cubic equations, such as the Cardano formula [84].

$$\begin{aligned}
k_{x1} &= \frac{\alpha}{2^{1/3}3^{2/3}} - \frac{2^{1/3}g}{3^{1/3}\alpha\gamma},\\
k_{x2} &= -\frac{\left(1-i\sqrt{3}\right)\alpha}{2\cdot 2^{1/3}3^{2/3}} + \frac{\left(1+i\sqrt{3}\right)g}{2^{2/3}3^{1/3}\alpha\gamma},\\
k_{x3} &= -\frac{\left(1+i\sqrt{3}\right)\alpha}{2\cdot 2^{1/3}3^{2/3}} + \frac{\left(1-i\sqrt{3}\right)g}{2^{2/3}3^{1/3}\alpha\gamma},\\
\alpha &= \left(\frac{9\omega^2\sqrt{1-N_\omega^2}}{\gamma} + \frac{\sqrt{3}\sqrt{4g^3-27N^2\gamma\omega^2+27\gamma\omega^4}}{\gamma^{3/2}}\right)^{1/3}.
\end{aligned} \tag{2.57}$$

Physically implemented roots are selected from solutions in Eq (2.57), which ensure the attenuation of motion with depth in Eqs (2.15), (2.23), and (2.29) for all flow components.

3. Results

We define wavelength λ of the regular solution and ligament δ_l scale of the singular solution as follows:

$$\lambda = \frac{2\pi}{\sqrt{\mathrm{Re}(k_x)^2 + \mathrm{Im}(k_z)^2}},$$
$$\delta_l = \frac{2\pi}{\sqrt{\mathrm{Re}(k_x)^2 + \mathrm{Im}(k_l)^2}}.$$

For weakly dissipative media, where the flow energy attenuates slowly, the relation $\nu k^2 \ll \omega$ holds true. For variables connected with the period of propagating perturbation and the spatial scales, the condition for ignoring energy dissipation can be written as:

$$\frac{\lambda^2}{\nu} \gg T, \qquad\qquad \frac{\delta_l^2}{\nu} \gg T. \tag{3.1}$$

The analysis shows that, for a liquid with water parameters, Eq (3.1) holds true for the values of the surface perturbation period $T > 2 \cdot 10^{-5}$ s. Thus, the ligament scale is of the order $\delta_l \sim 10^{-3}$ cm, and the wavelength is $\lambda \sim 5 \cdot 10^{-3}$ cm. This significantly exceeds the sizes of a molecular cluster $\delta_c \sim 10^{-6} \ldots 10^{-5}$ cm, at which the properties of a continuous medium emerge.

We construct the dispersion dependencies of all components of the surface capillary-gravitational periodic flows obtained in various formulations and approximations for a liquid with water properties $g = 981$ cm/s^2, $\sigma = 72$ erg/cm^2, and $\rho_{00} = 1$ g/cm^3 with different values of the buoyancy frequency $N = 1$ s^{-1}, which corresponds to a highly stratified liquid in laboratory conditions and $N = 0.01$ s^{-1}, which corresponds to a highly stratified ocean.

We introduce the following designations: Subscript "v" for variables obtained in the viscous fluid model, subscript "id" for variables in the ideal fluid model, superscript "f" for variables without the Boussinesq approximation, and superscript "b" for variables obtained in the model with the Boussinesq approximation.

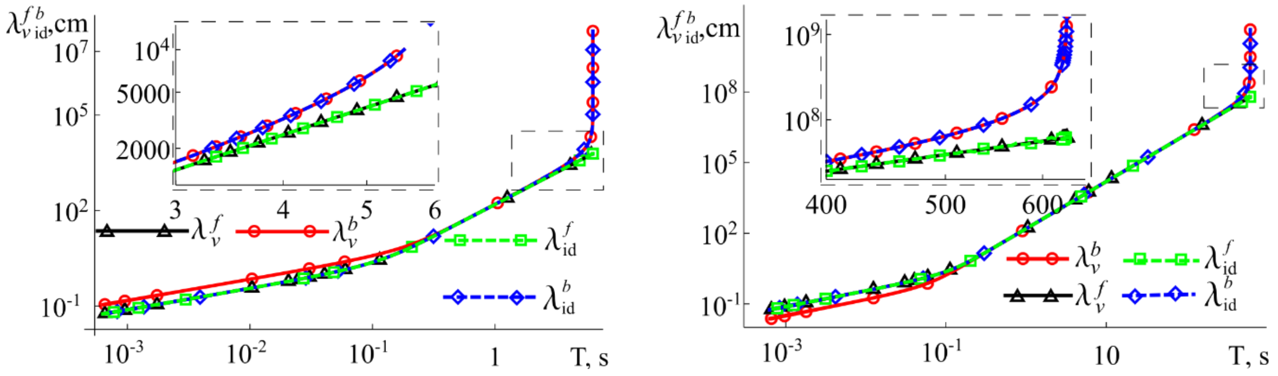

a) b)

Figure 1. Dependence of the wavelength on the period of the propagating perturbation in a highly stratified liquid in different models: a) In a stratified a laboratory liquid $N = 1\ \mathrm{s}^{-1}$; and b) in a highly stratified ocean $N = 0.01\ \mathrm{s}^{-1}$.

Figure 1 shows the dependences of the wavelength on the period of the propagating perturbation in a highly stratified fluid for different models. The models with the Boussinesq (i.e., with the approximation to buoyancy period T_b) show an unlimited increase in the wavelength. However, in the complete formulation, the wavelength remains finite and has values $\lambda_{T \to T_b} = 61.64$ m for a highly stratified laboratory liquid. Notably, for internal waves calculated in Eqs (2.22) and (2.25), the wavelength takes on the same value with the approximation of the perturbation period to the buoyancy period.

It is also worth noting that with the Boussinesq approximation in a viscous fluid, there is a deviation of the dispersion curve from the complete formulation for periodic flows with short periods corresponding to the capillary part of the spectrum. In a highly stratified laboratory fluid, the model employing the Boussinesq approximation may lead to an overestimation of the wavelength, while in a stratified ocean, it may result in an underestimation [76].

The wavelength in the ideal fluid model, without the Boussinesq approximation, practically coincides with the wavelength in the complete formulation. As the period of the propagating perturbation decreases, the ideal fluid model with the Boussinesq approximation predicts values that are close to those obtained in the complete formulation.

The value of the wavelength deviation calculated in different models is of particular interest. We denote the modulus of the difference between the values in the complete formulation and the viscous fluid model in the Boussinesq approximation with the subscript "fb", between the values in the complete formulation and the ideal fluid model with the index "fid", and between the values obtained in the complete formulation and the ideal fluid model with the Boussinesq approximation with the index "$fbid$".

Figure 2 shows the dependences of the modulus of the difference between the wavelengths in different models related to the wavelength on the propagating perturbation period, which is relative to the buoyancy period $\tilde{T} = T/T_b$ in the complete formulation. The relative difference between the wavelength in the complete formulation and in the Boussinesq approximation is indicated by $\tilde{\lambda}_{fb} = \Delta\lambda_{fb}/\lambda_f = \left|\lambda_v^f - \lambda_v^b\right|/\lambda_f$; between the complete formulation and in an ideal fluid model $\tilde{\lambda}_{fid} = \Delta\lambda_{fid}/\lambda_f = \left|\lambda_v^f - \lambda_{id}^f\right|/\lambda_f$; and between the complete formulation and in an ideal fluid with the Boussinesq approximation $\tilde{\lambda}_{fbid} = \Delta\lambda_{fbid}/\lambda_f = \left|\lambda_v^f - \lambda_{id}^b\right|/\lambda_f$:

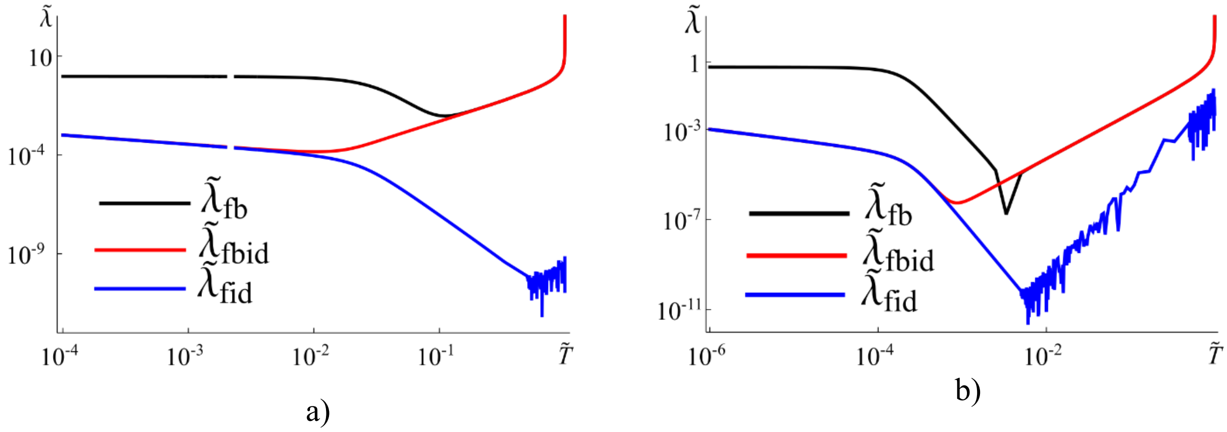

Figure 2. Dependences of the modulus of the difference between the wavelengths $\tilde{\lambda}$ on the relative period of the propagating perturbation $\tilde{T}$ in different models: a) In a stratified a laboratory liquid $N = 1$ s^{-1}; and b) in a highly stratified ocean $N = 0.01$ s^{-1}.

The analysis of the dependencies reveals that the difference in the description of regular surface flow component between the viscous fluid models (with or without the Boussinesq approximation) becomes noticeable when the ratios of the flow period to the medium buoyancy period are small $\tilde{T} = T/T_b \le 0.01$ for liquids with buoyancy frequencies $N = 1$ s^{-1} and $N = 0.01$ s^{-1}. As the ratio increases $\tilde{T}$, the difference decreases and reaches a minimum value $\tilde{\lambda}_{fb} = \Delta\lambda_{fb}/\lambda_f \simeq 0.009$ in a ratio of periods $\tilde{T} \simeq 0.11$ at $N = 1$ s^{-1}, and $\tilde{\lambda}_{fb} \simeq 10^{-7}$ in a ratio of periods $\tilde{T} \simeq 0.003$ at $N = 0.01$ s^{-1}. Then there is a sharp increase in the discrepancy between models, especially with the approximation of the flow period to the buoyancy period.

The dependence of the difference between the model in complete formulation and the ideal fluid model $\tilde{\lambda}_{fid} = \Delta\lambda_{fid}/\lambda_f$ is of special interest. The difference is negligible and amounts to only fractions of a percent at small ratios of the flow period to the medium buoyancy period $\tilde{T} \le 0.01$. It reaches its minimum value $\tilde{\lambda}_{fbid} = \Delta\lambda_{fbid}/\lambda_f \simeq 0.00015$ in the ratio of the periods $\tilde{T} \simeq 0.0104$ at $N = 1$ s^{-1}, and $\tilde{\lambda}_{fbid} \simeq 5\cdot 10^{-7}$ in the ratio of the periods $\tilde{T} \simeq 0.0009$ at $N = 0.01$ s^{-1}. With the approximation of the flow period to the buoyancy period, the difference in values of the regular flow component calculated in the model with complete formulation and in the ideal fluid model increases sharply.

The difference between the models that do not use the Boussinesq approximation is minimal, and with the approximation of the perturbation period to the fluid buoyancy period, the values are assumed to be $\tilde{\lambda}_{fid} < 10^{-3}$ over the range of observed periods of surface perturbations for the investigated liquids.

The situation is different for ligament components. In an ideal fluid model, there are no singular components, and it is impossible to obtain them; therefore, the comparison can be made only between the models of a viscous fluid with the Boussinesq approximation or in complete formulation. Calculations show that dependence of the singular ligament scale on the perturbation period in complete formulation δ_f^l and the Boussinesq approximation δ_b^l for a strongly stratified fluid with buoyancy frequency $N = 1\ \text{s}^{-1}$ described by the following relations:

$$\begin{aligned} \delta_f^l &\simeq 0.354572\sqrt{T} - 0.0005871,\ \text{cm}, \\ \delta_b^l &\simeq 0.354498\sqrt{T} - 0.0000175,\ \text{cm}. \end{aligned} \tag{3.2}$$

In a highly stratified ocean, $N = 0.01\ \text{s}^{-1}$ the dependence of the ligament scale on the period in various models can be expressed as follows:

$$\begin{aligned} \delta_f^l &\simeq 0.354494\sqrt{T} - 0.0000624,\ \text{cm}, \\ \delta_b^l &\simeq 0.354505\sqrt{T} - 0.0003248,\ \text{cm}. \end{aligned} \tag{3.3}$$

The differences between the characteristics obtained in different models in Eqs (3.2) and (3.3) are shown in Figures 3a) and 3b).

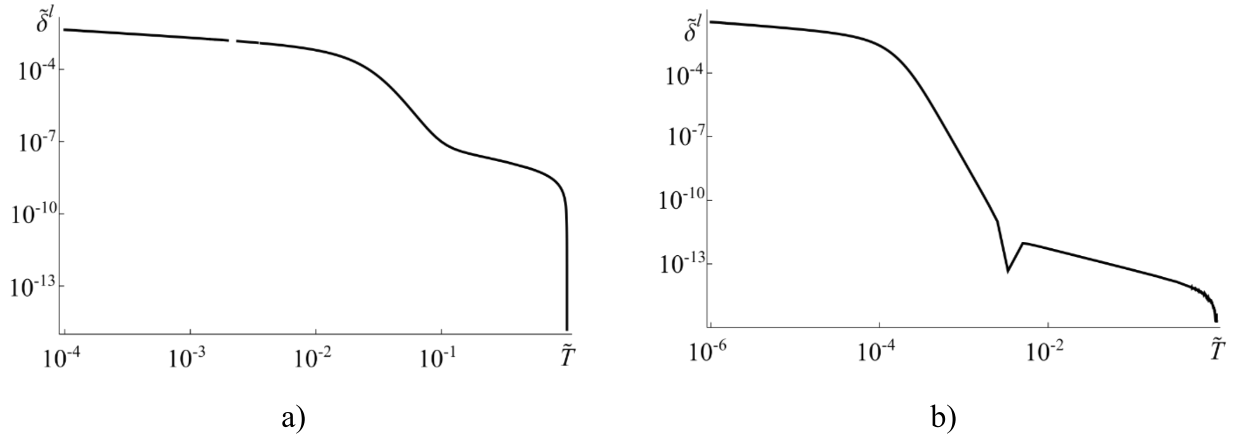

Figure 3. Dependences of the modulus of the difference between the ligament scales $\tilde{\delta}^l = \Delta\delta_{fb}^l / \delta_f^l = \left|\delta_f^l - \delta_b^l\right| / \delta_f^l$ in the complete formulation and in the Boussinesq approximation on the relative period of the propagating perturbation $\tilde{T}$: a) In a stratified laboratory fluid $N = 1\ \text{s}^{-1}$; and b) in a highly stratified ocean $N = 0.01\ \text{s}^{-1}$.

The difference between the characteristics of ligaments over a wide range of periods is only fractions of a percent and virtually disappears with the approximation to the buoyancy period.

The phase and group velocities, as well as their counterparts for ligamentous components, are of particular interest. Figure 4 illustrates the phase and group velocities of the regular wave component of periodic flow in a stratified laboratory fluid $N=1\ \text{s}^{-1}$, depending on the period, which are calculated in various approximations.

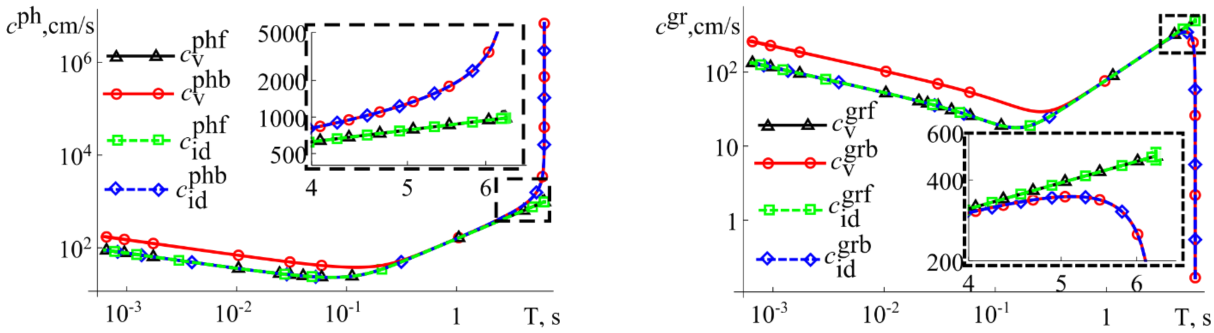

a) b)

Figure 4. a) Phase velocities and b) group velocities of the wave component of a periodic flow in various models.

Analyzing the graphs of the group and phase velocities, we can conclude that for small periods (corresponding to the capillary part of the spectrum), the ideal fluid model has the best agreement with the problem in complete formulation. With the approximation of the buoyancy period, the models with the Boussinesq approximation show an unlimited increase in phase velocity and a tendency toward zero values of group velocity. This is not true for the model in complete formulation.

The differences between the phase and group velocities of the wave component in a stratified laboratory fluid $N=1\ \text{s}^{-1}$, obtained in complete formulation and in the Boussinesq approximation $\tilde{c}_{fb}^{ph}=\Delta c_{fb}^{ph}/c_f^{ph}=\left|c_f^{ph}-c_b^{ph}\right|/c_f^{ph}$ and $\tilde{c}_{fb}^{gr}=\Delta c_{fb}^{gr}/c_f^{gr}=\left|c_f^{gr}-c_b^{gr}\right|/c_f^{gr}$ in complete formulation and in an ideal fluid model $\tilde{c}_{fid}^{ph}=\Delta c_{fid}^{ph}/c_f^{ph}=\left|c_f^{ph}-c_{id}^{ph}\right|/c_f^{ph}$ and $\tilde{c}_{fid}^{gr}=\Delta c_{fid}^{gr}/c_f^{gr}=\left|c_f^{gr}-c_{id}^{gr}\right|/c_f^{gr}$ in the Boussinesq approximation in a viscous and in an ideal fluids $\tilde{c}_{bid}^{ph}=\Delta c_{bid}^{ph}/c_f^{ph}=\left|c_b^{ph}-c_{id}^{ph}\right|/c_f^{ph}$ and $\tilde{c}_{bid}^{gr}=\Delta c_{bid}^{gr}/c_f^{gr}=\left|c_b^{gr}-c_{id}^{gr}\right|/c_f^{gr}$ are shown in Figure 5.

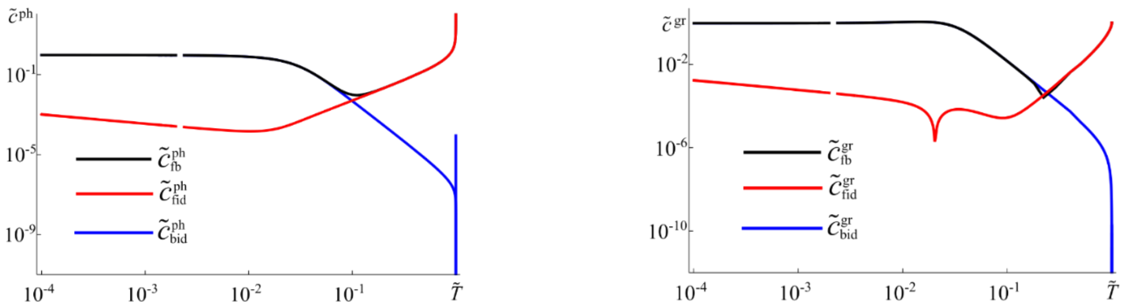

a) b)

Figure 5. Relative differences between a) phase $\tilde{c}^{ph}$ and b) group $\tilde{c}^{gr}$ velocities on the relative period of the propagating perturbation $\tilde{T}$.

It is not difficult to calculate the analog of the phase velocity for the ligament:

$$c^{lph} = \frac{\delta^l}{T}. \tag{3.4}$$

Then, for different models, considering Eqs (3.2) and (3,3), simple analytical expressions are obtained for a highly stratified fluid $N = 1\ \mathrm{s}^{-1}$:

$$\begin{aligned} c_f^{lph} &\simeq \frac{0.354572}{\sqrt{T}} - \frac{0.0005871}{T}, \mathrm{cm/s}, \\ c_b^{lph} &\simeq \frac{0.354498}{\sqrt{T}} - \frac{0.0000175}{T}, \mathrm{cm/s}. \end{aligned} \tag{3.5}$$

For a stratified ocean:

$$\begin{aligned} c_f^{lph} &\simeq \frac{0.354494}{\sqrt{T}} - \frac{0.0000624}{T}, \mathrm{cm/s}, \\ c_b^{lph} &\simeq \frac{0.354505}{\sqrt{T}} - \frac{0.0003248}{T}, \mathrm{cm/s}. \end{aligned} \tag{3.6}$$

Similarly, analytical expressions can be derived for the analog of the ligament group velocity:

$$c^{\lg r} = \frac{d\delta^l}{dT}. \tag{3.7}$$

Using Eqs (3.2), (3.3), (3.5), and (3.6), we present expressions for ligament group velocities calculated in the complete model $c_f^{\lg r}$ and in the Boussinesq approximation $c_b^{\lg r}$ for a highly stratified fluid $N = 1\ \mathrm{s}^{-1}$:

$$\begin{aligned} c_f^{\lg r} &\simeq \frac{0.178786}{\sqrt{T}}, \mathrm{cm/s}, \\ c_b^{\lg r} &\simeq \frac{0.177249}{\sqrt{T}}, \mathrm{cm/s}. \end{aligned} \tag{3.8}$$

For a stratified ocean, we can derive the expressions for group velocities as follows:

$$\begin{aligned} c_f^{\lg r} &\simeq \frac{0.177247}{\sqrt{T}}, \mathrm{cm/s}, \\ c_b^{\lg r} &\simeq \frac{0.177253}{\sqrt{T}}, \mathrm{cm/s}. \end{aligned} \tag{3.9}$$

The differences in the phase and group velocity values of the ligament components, calculated in the model with the Boussinesq approximation and in complete formulation, are almost negligible. To illustrate this, Figure 6 shows the relative differences in phase and group velocities, depending on the period of the propagating flow, which is attributed to the buoyancy period.

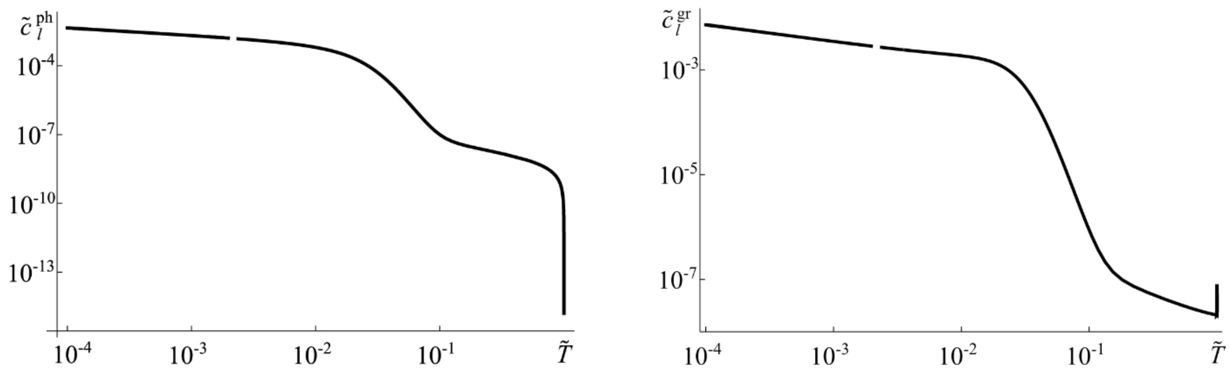

a) b)

Figure 6. Relative differences between a) phase $\tilde{c}_l^{ph} = \Delta c_{fb}^{lph} / c_f^{lph} = \left|c_f^{lph} - c_b^{lph}\right| / c_f^{lph}$ and b) group $\tilde{c}_l^{gr} = \Delta c_{fb}^{lgr} / c_f^{lgr} = \left|c_f^{lgr} - c_b^{lgr}\right| / c_f^{lgr}$ velocities in complete formulation and the Boussinesq approximation for the ligament component of the periodic flow on the relative period of the propagating perturbation $\tilde{T}$.

The greatest differences in characteristics are observed for small values of periods in the capillary domain of the spectrum for ligament components in contrast to wave components. With the approximation to the buoyancy period, these differences practically disappear.

The non-monotonic nature of the differences in characteristics is worth mentioning. The graphs of the relative difference between the phase and group velocities of regular wave components show a local minimum in the middle of the spectrum, corresponding to capillary gravitational waves. However, there is an inflection point in this domain for ligament components. The steepness of the curve changes significantly, but the overall tendency remains the same, i.e., the relative difference of velocities calculated in different models decreases as the period of the propagating perturbation increases.

4. Discussion

The methodology developed in this paper enables us to determine complete solutions that correspond to the employed mathematical model. These complete solutions consist of regular components, which, in limiting cases, are uniformly reduced to known expressions for waves on the surface of a heavy liquid, taking into account surface tension. They also contain singular components, which disappear in the ideal fluid model and define new flow elements that are ligaments, forming the fine structure of viscous liquids.

The construction of a solution based on the fundamental system of fluid mechanics equations leads to a greater number of singular solutions that determine the structural components of the flow, which are connected with temperature and chemical composition heterogeneity. The ideal fluid model does not include fine-structured components. Therefore, we can assume that an ideal fluid does not comprise the most widespread component of flows, and the ideal fluid models should be employed with caution, considering their limitations.

To observe fine structures in an experiment, it is necessary to use high-resolution laboratory equipment. The parameters of this equipment can be calculated based on theoretical results presented in this paper, which are based on the intrinsic scales of the problem taking into account the medium characteristics.

In the 3D formulation, the order of the system of equations increases, and two solutions belonging to the singular class are added. Obtaining complete solutions in the 3D formulation is complicated by the fact that, even within the incompressible fluid model, it is impossible to reduce the expressions to an equation for a single scalar function analogous to the stream function in the 2D formulation. A possible way out of these difficulties is to use the toroidal–poloidal decomposition [85], in which the velocity $\mathbf{u} = (u, v, w)$ is expressed through the toroidal T and poloidal Π components:

$$\mathbf{u} = \nabla \times \left(\mathrm{T}(\mathbf{r}, t) \cdot \mathbf{e}_z\right) + \nabla \times \nabla \times \left(\Pi(\mathbf{r}, t) \cdot \mathbf{e}_z\right). \tag{4.1}$$

Analysis of the expressions shows that representation in Eq (4.1) automatically satisfies the fluid incompressibility condition. Its use makes it possible to split the problem into separate equations for the toroidal and poloidal components of three-dimensional flows. The expressions imply the existence of additional singular solutions describing ligament components that are new compared to the 2D formulation. A detailed analysis of the complete solutions in the 3D formulation is a separate problem, the solution of which may be found using a united theory of regular and singular perturbations.

5. Conclusions

Based on the fundamental system of equations for fluid mechanics, a reduced problem on the propagation of surface and internal gravitational periodic perturbations in a viscous, uniformly stratified liquid is formulated. For the first time, complete analytical solutions of the equations of motion in a spectral form are obtained asymptotically for a fluid model that does not employ additional simplifying assumptions. It is shown that in the viscous fluid model, qualitatively new terms describing the fine structure of flows are determined by the singular solutions of the spectral form of the governing equations.

Complete solutions to the reduced system of fundamental equations in a 2D formulation have been obtained. Abandoning the Boussinesq approximation leads to the appearance of additional terms. The form of these additional terms indicates a strong dependence of the solutions on the initial and boundary conditions. In the complete formulation of the problem, it is necessary to pose the problem of the propagation of all components of periodic flows in heterogeneous fluids, taking into account physically substantiated initial and boundary conditions. A 2D dispersion relation that considers the presence of a free fluid surface is derived, and the solution to the dispersion equation is analyzed using numerical methods. Comparisons are made between simpler models for analytical and numerical calculations for different values of problem parameters. Ranges of periods and linear scales for the components of periodic flows are identified, which determine the minimum deviation of simple models from the complete one, indicating deviation values. Moreover, relations for the phase and group velocities of surface waves and their counterparts for structural components (ligaments) are derived. The expressions and relations obtained can be verified experimentally using high-resolution tools in spatial and temporal coordinates.

Use of AI tools declaration

The authors declare they have not used Artificial Intelligence (AI) tools in the creation of this article.

Acknowledgments

The study was supported by the Government program (contract #124012500442-3).

Conflict of interest

Prof. Yuli D. Chashechkin is an editorial board member for Networks and Heterogeneous Media and was not involved in the editorial review or the decision to publish this article. All authors declare that there are no competing interests.

Author contributions

Yuli D. Chashechkin: Conceptualization, Methodology (equal), Formal analysis (equal), Writing original draft, review and editing (equal). Artem A. Ochirov: Methodology (equal), Investigation, Formal analysis (equal), Writing original draft, review and editing (equal).

References

1. K. N. Fedorov, *The Thermohaline Finestructure of the Ocean*, Pergamon Marine Series, J. C. Swallow (1st ed), Elsevier, Amstrdam, Netherlands, 2013. https://doi.org/10.1016/C2013-0-02890-3
2. US Standard Atmosphere, NOAA-S/T-76-1562, NASA-TM-X-74335, Accession No. 77N16482, 1976. Available from: https://ntrs.nasa.gov/citations/19770009539.
3. I. P. Chunchuzov, S. N. Kulichkov, *Infrasound Propagation in an Anisotropic Fluctuating Atmosphere*, Cambridge Scholars Publishing, London, 2020. https://doi.org/10.65325/EB8133
4. L. Prandtl, *Guide to Fluid Mechanics*, Friedr. Vieweg & Sohn, Braunschweig, Germany, 1942.
5. A. V. Kistovich, Yu. D. Chashechkin, The structure of transient boundary flow along an inclined plane in a continuously stratified medium, *J. Appl. Mech.*, **57** (1993), 633–639. https://doi.org/10.1016/0021-8928(93)90033-I
6. J. S. Turner, *Buoyancy Effects in Fluids*, Cambridge University Press (CUP), Cambridge, UK, 1980. https://doi.org/10.1017/CBO9780511608827
7. Y. D. Chashechkin, Discrete and continuous symmetries of stratified flows past a sphere, *Symmetry*, **14** (2022), 1278. https://doi.org/10.3390/sym14061278
8. D. Eisenberg, W. Kauzmann, *The Structure and Properties of Water*, Oxford University Press, Oxford, 2005. https://doi.org/10.1093/acprof:oso/9780198570264.001.0001
9. G. G. Malenkov, Structure and dynamics of surfaces of thin films and water microdroplets, *Colloid J.*, **72** (2010), 653–662. https://doi.org/10.1134/S1061933X1005011X
10. R. Feistel, Thermodynamic properties of seawater, ice and humid air: TEOS-10, before and beyond, *Ocean Sci.*, **14**, (2018), 471–502. https://doi.org/10.5194/os-14-471-2018

11. A. H. Harvey, J. Hrubý, K. Meier, Improved and always improving: Reference formulations for thermophysical properties of water, *J. Phys. Chem. Ref. Data*, **52** (2023), 011501. https://doi.org/10.1063/5.0125524
12. Y. D. Chashechkin, Foundations of engineering mathematics applied for fluid flows, *Axioms,* **10** (2021), 286. https://doi.org/10.3390/axioms10040286
13. D. L. Parfinenko, Studies of the fine structure of the solar photosphere at Pulkovo Observatory, *Geomagn. Aeron.*, **61** (2021), 949–955. https://doi.org/10.1134/S001679322107015X
14. L. Euler, *General Principles of the Motion of Fluids*, Mémoires de l'Académie Royale des Sciences et des Belles-Lettres de Berlin, **11** (1757), 274–315.
15. G. G. Stokes, *On the Theories of the Internal Friction of Fluids in Motion, and of the Equilibrium and Motion of Elastic Solids*, Mathematical and Physical Papers, Cambridge Library Collection-Mathematics, Cambridge University Press, Cambridge, UK, 2009, 75–129. https://doi.org/10.1017/CBO9780511702242.005
16. N. E. Kochin, I. A. Kibel, N. V. Roze, *Theoretical Hydromechanics*, Interscience Publishers, New York, 1964. Available from: https://archive.org/details/theoreticalhydro0000koch/page/n5/mode/2up.
17. L. D. Landau, E. M. Lifshitz, *Fluid Mechanics: Course of Theoretical Physics*, Pergamon Press, Oxford, UK, 1987. https://doi.org/10.1016/C2013-0-03799-1
18. G. G. Stokes, *On the Effect of Internal Friction of Fluids on the Motion of Pendulums*, Mathematical and Physical Papers, Cambridge Library Collection-Mathematics, Cambridge University Press, Cambridge, UK, 2009, 1–10. https://doi.org/10.1017/CBO9780511702266.002
19. G. G. Stokes, *On the Theory of Oscillatory Waves*, Mathematical and Physical Papers, Cambridge Library Collection-Mathematics, Cambridge University Press, Cambridge, UK, 2009, 197–229. https://doi.org/10.1017/CBO9780511702242.013
20. H. Lamb, *Hydrodynamics (Sixth edition*), Cambridge University Press (CUP), Cambridge, UK, 1932. Available from: https://assets.cambridge.org/97805214/58689/frontmatter/9780521458689_frontmatter.pdf.
21. B. Franklin, Behavior of oil on water (letter to J. Pringle), in *Experiments and Observations on Electricity*, R. Cole, London, UK, 1769, 142–144. Available from: https://archive.org/details/experimentsobser00fran_0/page/n3/mode/2up.
22. V. W. Ekman, On dead water, in *The Norwegian North Polar Expedition 1893–1896. Scientific results*, F. Nansen, (ed.), Christiania, Norway, 1906. Available from: https://archive.org/download/norwegiannorthpo05nans/norwegiannorthpo05nans.pdf.
23. L. Rayleigh, Investigation of the character of the equilibrium of an incompressible heavy fluid of variable density, *Proc. Lond. Math. Soc.*, **114** (1882), 170–177. https://doi.org/10.1112/plms/s1-14.1.170
24. V. Väisälä, On the effect of wind fluctuations on pilot balloon observations, in *Societas Scientiarum Fennicae Commentationes Physico-Mathematicae*, **2** (1925), 19–37.
25. D. Brunt, The period of simple vertical oscillations in the atmosphere, *Q. J. R. Meteorol. Soc.*, **53** (1927), 30–32. https://doi.org/10.1002/qj.49705322103
26. H. Lamb, On atmospheric oscillations, *Proc. A*, **84** (1911), 551–572. https://doi.org/10.1098/RSPA.1911.0008

27. J. M. Lighthill, *Waves in Fluids: Cambridge Mathematical Library*, Cambridge University Press (CUP), Cambridge, UK, 1978. Available from: https://www.cambridge.org/gb/universitypress/subjects/mathematics/fluid-dynamics-and-solid-mechanics/waves-fluids-1?format=PB&isbn=9780521010450.
28. I. Tolstoy, C. S. Clay, *Ocean Acoustics: Theory and Experiment in Underwater Sound*, McGraw-Hill Book Company, New York, NY, USA, 1966. Available from: https://archive.org/details/oceanacoustics00ivan/page/n5/mode/2up.
29. A. H. Nayfeh, *Introduction to Perturbation Technique*, John Wiley & Sons, New York, USA, 1993.
30. S. Dio Ranandrasana, L. Zhang, M. M. Bhatti, M. Marin, Study of Jeffrey fluid motion through irregular porous circular microchannel under the implications of electromagnetohydrodynamic and surface charge-dependent slip, *Mathematics*, **14** (2026), 722. https://doi.org/10.3390/math14040722
31. S. G. Teoh, G. N. Ivey, J. Imberger, Laboratory study of the interaction between two internal wave rays, *J. Fluid Mech.*, **336** (1997), 91–122. https://doi.org/10.1017/S0022112096004508
32. A. D. McEwan, Interactions between internal gravity waves and their traumatic effect on a continuous stratication, *Boundary-Layer Met.*, **5** (1973), 159–175. https://doi.org/10.1007/BF02188317
33. Yu. V. Kistovich, Yu. D. Chashechkin, An exact solution of a linearized problem of the radiation of monochromatic internal waves in a viscous fluid, *J. Appl. Math. Mech.*, **63** (1999), 587–594. https://doi.org/10.1016/S0021-8928(99)00073-8
34. Yu. D. Chashechkin, Yu. V. Kistovich, S. A. Smirnov, Linear generation theory of 2D and 3D periodic internal waves in a viscous stratified fluid, *Environmetrics*, **12** (2001), 57–80. https://doi.org/10.1002/1099-095X(200102)12:1<57::AID-ENV446>3.0.CO;2-1
35. L. Rayleigh, Some applications of photography, *Nature*, **44** (1891), 249–254. https://doi.org/10.1038/044249e0
36. Y. V. Kistovich, Y. D. Chashechkin, Linear theory of the propagation of internal wave beams in an arbitrarily stratified liquid September, *J. Appl. Mech. Tech. Phys.*, **39** (1998), 729–737. https://doi.org/10.1007/BF02468043
37. M. S. Paoletti, H. L. Swinney, Propagating and evanescent internal waves in a deep ocean model, *J. Fluid Mech.*, **706** (2012), 571–583. https://doi.org/10.1017/jfm.2012.284
38. G. B. Airy, *Encyclopaedia Metropolitana: Tides and Waves*, B. Fellowes, London, UK, 1845.
39. L. N. Sretenskii, *Theory of Wave Motions of a Liquid*, ONTI (United Scientific and Technical Publishing House), Moscow–Leningrad, USSR, 1936.
40. G. B. Whitham, *Linear and Nonlinear Waves (Pure and Applied Mathematics Series)* Wiley-Interscience, New York, 1974. https://doi.org/10.1002/9781118032954
41. O. M. Phillips, *The Dynamics of the Upper Ocean*, 2nd edition, Cambridge University Press, Cambridge, UK, 1977.
42. P. H. LeBlond, L. A. Mysak, *Waves in the Ocean*, Elsevier Oceanography Series, Elsevier, Amsterdam, New York, 1978. Available from: https://www.sciencedirect.com/bookseries/elsevier-oceanography-series/vol/20/suppl/C.
43. R. G. Dean, R. A. Dalrymple, *Water Wave Mechanics for Engineers and Scientists*, Advanced Series on Ocean Engineering, World Scientific Publishing Company, Singapore, **2** (1991). https://doi.org/10.1142/1232

44. S. R. Massel, *Ocean Surface Waves: Their Physics and Prediction*, Advanced Series on Ocean Engineering, World Scientific Publishing Co. Pte Ltd, Singapore, **11** (1996). https://doi.org/10.1142/2285
45. J. J. Stoker, *Water Waves: The Mathematical Theory with Applications*, Wiley, New York, 1957. https://doi.org/10.1002/9781118033159
46. A. G. Davies, A. D. Heathershaw, Surface-wave propagation over sinusoidally varying topography, *J. Fluid Mech.*, **144** (1984), 419–443. https://doi.org/10.1017/S0022112084001671
47. A. D. D. Craik, *Wave Interactions and Fluid Flows*, Cambridge University Press, Cambridge, UK, 1988. https://doi.org/10.1017/CBO9780511569548
48. T. H. Havelock, The pressure of water waves upon a fixed obstacle, *Proc. A*, **175** (1940), 409–421. https://doi.org/10.1098/rspa.1940.0066
49. F. Ursell, The effect of a fixed vertical barrier on surface waves in deep water, *Math. Proc. Camb. Philos. Soc.*, **43** (1947), 374–382. https://doi.org/10.1017/S0305004100023604
50. W. R. Dean, On the reflexion of surface waves by a submerged plane barrier, *Math. Proc. Camb. Philos. Soc.*, **41** (1945), 231–238. https://doi.org/10.1017/S030500410002260X
51. R. Porter, D. V. Evans, Complementary approximations to wave scattering by vertical barriers, *J. Fluid Mech.*, **294** (1995), 155–180. https://doi.org/10.1017/S0022112095002849
52. A. J. Li, Y. Liu, H. J. Li, Accurate solutions to water wave scattering by vertical thin porous barriers, *Math. Probl. Eng.*, 2015, 985731. https://doi.org/10.1155/2015/985731
53. H. Y. Lo, P. L. F. Liu, On the analytical solutions for water waves generated by a prescribed landslide, *J. Fluid Mech.*, **821** (2017), 85–116. https://doi.org/10.1017/jfm.2017.251
54. A. Li, Y. Liu, New analytical solutions to water wave diffraction by vertical truncated cylinders, *Int. J. Nav. Archit. Ocean Eng.*, **11** (2019), 952–969. https://doi.org/10.1016/j.ijnaoe.2019.04.006
55. J. Shelton, P. Milewski, P. H. Trinh, Time-dependent nonlinear gravity-capillary surface waves with viscous dissipation and wind forcing, *J. Fluid Mech.*, **1003** (2025), A13. https://doi.org/10.1017/jfm.2024.1227
56. S. H. Choi, Weighted energy method and long wave short wave decomposition on the linearized compressible Navier–Stokes equation, *Networks Heterog. Media*, **8** (2013), 465–479. https://doi.org/10.3934/nhm.2013.8.465
57. B. P. Andreianov, F. Lagoutière, N. Seguin, T. Takahashi, Small solids in an inviscid fluid, *Networks Heterog. Media*, **5** (2010), 385–404. https://doi.org/10.3934/nhm.2010.5.385
58. M. Berezhnyi, L. Berlyand, E. Khruslov, The homogenized model of small oscillations of complex fluids, *Networks Heterog. Media*, **3** (2008), 831–862. https://doi.org/10.3934/nhm.2008.3.831
59. Z. Yang, P. L. F. Liu, New 2-D horizontal free-surface-flow models with applications for water waves, *J. Fluid Mech.*, **999** (2024), A32. https://doi.org/10.1017/jfm.2024.604
60. Y. He, A. Slunyaev, N. Mori, A. Chabchoub, Experimental evidence of nonlinear focusing in standing water waves, *Phys. Rev. Lett.*, **129** (2022), 144502. https://doi.org/10.1103/PhysRevLett.129.144502
61. M. Maleewong, R. Grimshaw, Evolution of water wave groups with wind action, *J. Fluid Mech.*, **947** (2022), A35. https://doi.org/10.1017/jfm.2022.675
62. S. V. Filatov, V. M. Parfenyev, S. S. Vergeles, M. Y. Brazhnikov, A. A. Levchenko, V. V. Lebedev, Nonlinear generation of vorticity by surface waves, *Phys. Rev. Lett.*, **116** (2016), 054501. https://doi.org/10.1103/PhysRevLett.116.054501

63. C. Bingol, M. Duran-Matute, R. Zhu, E. Meiburg, H. J. Clercx, Gravity currents under oscillatory forcing, *J. Fluid Mech.*, **1002** (2025), A14. https://doi.org/10.1017/jfm.2024.1170
64. M. Marino, M. Stagnitti, L. M. Stancanelli, R. E. Musumeci, E. Foti, Dynamics of wave-supported gravity currents in intermediate water, *Cont. Shelf Res.*, **267** (2023), 105082. https://doi.org/10.1016/j.csr.2023.105082
65. Y. Qiao, H. Wen, S. Evje, Compressible and viscous two-phase flow in porous media based on mixture theory formulation, *Networks Heterog. Media*, **14** (2019), 489–536. https://doi.org/10.3934/nhm.2019020
66. Y. Tai, X. Wang, W. Yin, P. Meng, Weak Galerkin method for the Navier–Stokes equation with nonlinear damping term, *Networks Heterog. Media*, **19** (2024), 475–499. https://doi.org/10.3934/nhm.2024021
67. N. Aïssiouene, M. O. Bristeau, E. Godlewski, J. Sainte-Marie, A combined finite volume-finite element scheme for a dispersive shallow water system, *Networks Heterog. Media*, **11** (2016), 1–27. https://doi.org/10.3934/nhm.2016.11.1
68. J. H. He, Homotopy perturbation technique, *Comput. Methods Appl. Mech. Eng.*, **178** (1999), 257–262. https://doi.org/10.1016/S0045-7825(99)00018-3
69. G. M. Moatimid, M. A. A. Mohamed, K. Elagamy, A Casson nanofluid flow within the conical gap between rotating surfaces of a cone and a horizontal disc, *Sci. Rep.*, **12** (2022), 11275 https://doi.org/10.1038/s41598-022-15094-w
70. G. M. Moatimid, M. A. A. Mohamed, K. Elagamy, Prandtl-Eyring couple stressed flow within a porous region counting homogeneous and heterogeneous reactions across a stretched porous sheet, *Partial Differ. Equ. Appl. Math.*, **10** (2024), 100706. https://doi.org/10.1016/j.padiff.2024.100706
71. G. M. Gie, M. Hamouda, R. Temam, Asymptotic analysis of the Navier–Stokes equations in a curved domain with a non-characteristic boundary, *Networks Heterog. Media*, **7** (2012), 741–766. https://doi.org/10.3934/nhm.2012.7.741
72. K. Matsuda, S. Komori, N. Takagaki, R. Onishi, Effects of surface tension reduction on wind-wave growth and air–water scalar transfer, *J. Fluid Mech.*, **960** (2023), A22. https://doi.org/10.1017/jfm.2023.144
73. X. Hong, G. Zheng, R. Cai, Y. Chen, G. Xiao, Computational fluid dynamics prediction of the sea-keeping behavior of high-speed unmanned surface vehicles under the coastal intersecting waves, *J. Mar. Sci. Eng.*, **13** (2025), 83. https://doi.org/10.3390/jmse13010083
74. X. Yu, D. L. Yi, P. Wang, Enhancing ocean temperature and salinity reconstruction with deep learning: The role of surface waves, *J. Mar. Sci. Eng.*, **13** (2025), 910. https://doi.org/10.3390/jmse13050910
75. Y. D. Chashechkin, A. A. Ochirov, Periodic waves and ligaments on the surface of a viscous exponentially stratified fluid in a uniform gravity field, *Axioms*, **11** (2022), 402. https://doi.org/10.3390/axioms11080402
76. A. A. Ochirov, Y. D. Chashechkin, Two-dimensional surface periodic flows of an incompressible fluid in various models of the medium, *Izv. Atmos. Ocean. Phys.*, **60** (2024), 1–14, https://doi.org/10.1134/S0001433824700087
77. C. M. Bender, S. A. Orszag, *Advanced Mathematical Methods for Scientists and Engineers I: Asymptotic Methods and Perturbation Theory*, Springer New York, NY, 1999. https://doi.org/10.1007/978-1-4757-3069-2

78. P. Muller, *The Equations of Oceanic Motions*, Cambridge University Press (CUP), Cambridge, UK, 2006. https://doi.org/10.1017/CBO9780511617843
79. L. F. McGoldrick, On the rippling of small waves: A harmonic nonlinear nearly resonant interaction, *J. Fluid Mech.*, **52** (1972), 725–751. https://doi.org/10.1017/S0022112072002733
80. A. H. Nayfeh, Third-harmonic resonance in the interaction of capillary and gravity waves, *J. Fluid Mech.*, **48** (1971), 385–395. https://doi.org/10.1017/S0022112071001630
81. D. D. Joseph, Domain perturbations: The higher order theory of infinitesimal water waves, *Arch. Ration. Mech. Anal.*, **51** (1973), 295–303. https://doi.org/10.1007/BF00250536
82. A. N. Colli, J. M. Bisang, Exploring the impact of concentration and temperature variations on transient natural convection in metal electrodeposition: A finite volume method analysis, *J. Electrochem. Soc.*, **170** (2023), 083505. https://doi.org/10.1149/1945-7111/acef62
83. D. J. Tritton, *Physical Fluid Dynamics*, Springer Dordrecht, 1977. https://doi.org/10.1007/978-94-009-9992-3
84. J. Stillwell, J. Stillwell, *Mathematics and Its History*, Springer New York, NY, 1989. https://doi.org/10.1007/978-1-4899-0007-4
85. S. Chandrasekhar, *Hydrodynamic and Hydromagnetic Stability*, Clarendon Press (Oxford University Press), Oxford, UK, 1961.